

## San Jose State University SJSU ScholarWorks

---

Master's Theses

Master's Theses and Graduate Research

---

1996

# Impedance control

Kevin Kamal Mapar  
*San Jose State University*

Follow this and additional works at: [https://scholarworks.sjsu.edu/etd\\_theses](https://scholarworks.sjsu.edu/etd_theses)

---

### Recommended Citation

Mapar, Kevin Kamal, "Impedance control" (1996). *Master's Theses*. 1321.  
DOI: <https://doi.org/10.31979/etd.chy2-5twy>  
[https://scholarworks.sjsu.edu/etd\\_theses/1321](https://scholarworks.sjsu.edu/etd_theses/1321)

This Thesis is brought to you for free and open access by the Master's Theses and Graduate Research at SJSU ScholarWorks. It has been accepted for inclusion in Master's Theses by an authorized administrator of SJSU ScholarWorks. For more information, please contact [scholarworks@sjsu.edu](mailto:scholarworks@sjsu.edu).

## INFORMATION TO USERS

This manuscript has been reproduced from the microfilm master. UMI films the text directly from the original or copy submitted. Thus, some thesis and dissertation copies are in typewriter face, while others may be from any type of computer printer.

**The quality of this reproduction is dependent upon the quality of the copy submitted.** Broken or indistinct print, colored or poor quality illustrations and photographs, print bleedthrough, substandard margins, and improper alignment can adversely affect reproduction.

In the unlikely event that the author did not send UMI a complete manuscript and there are missing pages, these will be noted. Also, if unauthorized copyright material had to be removed, a note will indicate the deletion.

Oversize materials (e.g., maps, drawings, charts) are reproduced by sectioning the original, beginning at the upper left-hand corner and continuing from left to right in equal sections with small overlaps. Each original is also photographed in one exposure and is included in reduced form at the back of the book.

Photographs included in the original manuscript have been reproduced xerographically in this copy. Higher quality 6" x 9" black and white photographic prints are available for any photographs or illustrations appearing in this copy for an additional charge. Contact UMI directly to order.

# UMI

A Bell & Howell Information Company  
300 North Zeeb Road, Ann Arbor MI 48106-1346 USA  
313/761-4700 800/521-0600



# IMPEDANCE CONTROL

A Thesis

Presented to

The Faculty of the Department of Mechanical Engineering  
San Jose State University

In Partial Fulfillment  
of the Requirements for the Degree  
Master of Science

by

Kevin Kamal Mapar

August 1996

**UMI Number: 1381432**

---

**UMI Microform 1381432**  
**Copyright 1996, by UMI Company. All rights reserved.**

**This microform edition is protected against unauthorized  
copying under Title 17, United States Code.**

---

**UMI**  
**300 North Zeeb Road**  
**Ann Arbor, MI 48103**

© 1996


Kevin Kamal Mapar

ALL RIGHTS RESERVED

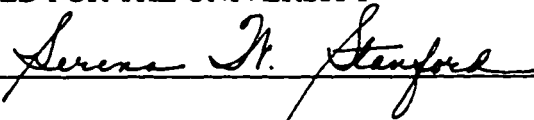
APPROVED FOR THE DEPARTMENT OF MECHANICAL ENGINEERING

  
\_\_\_\_\_  
Dr. Imin Kao

  
\_\_\_\_\_  
Dr. Ji C. Wang

  
\_\_\_\_\_  
Dr. William Seto

APPROVED FOR THE UNIVERSITY

  
\_\_\_\_\_

# Abstract

This thesis reviews two different approaches often employed in the field of impedance control: position based impedance control and force based impedance control. This work considers the non-ideal, practical effects of environmental parameters and manipulator dynamics on the behaviors of the two primary approaches to impedance control. The results are cast in the form of stability boundaries - the relationship between desired impedance parameters - which cause marginally stable behavior in the overall system. These stability boundaries are compared for the two primary implementations and relative advantages of each approach are discussed. These comparisons provide the basis for selection of control implementation approaches suited for particular manipulator, and allow quantitative decisions to be made in manipulator system design. The type of testing to be performed for the system to verify the dynamic math model is specified and presented. The validity of the implemented system is investigated by performing a series of tests with a Schilling manipulator.



# Table of Contents

Abstract .....	iv
List of figures .....	vii
Acronyms.....	viii
1.0 Introduction .....	1
1.1 Introduction and background .....	1
1.2 Preview and outline of the following chapters.....	2
1.3 Terminology and notations.....	3
2.0 Literature review.....	4
2.1 Introduction .....	4
2.2 Hybrid position/force control .....	5
2.3 Impedance control.....	7
3.0 Impedance control.....	9
3.1 Introduction .....	9
3.2 Preliminaries .....	10
3.2.1 Position based impedance control.....	13
3.2.2 Torque based impedance control.....	22
3.3 summary.....	25
4.0 Controller design and experimental results.....	27
4.1 Introduction .....	27
4.2 Preliminaries .....	27
4.2.1 The dynamic models.....	28
4.2.2 The conventional impedance control.....	28

4.3 The control algorithm .....	30
4.3.1 Impedance control with estimate dynamics .....	30
4.3.2 The target impedance reference trajectory .....	31
4.4 Experimental results.....	33
4.4.1 Experimental setup.....	33
4.4.2 Experimental verification of target dynamics .....	36
4.5 Conclusion .....	39
5.0 Conclusion and future work .....	51
5.1 Conclusion .....	51
5.2 Future work.....	52
Appendix A.....	53
Bibliography and references.....	57

# List of Figures

Figure 2-1 Block diagram of one-dimensional force control system.....	7
Figure 3-1 Position based model along a single Cartesian degree of freedom.....	21
Figure 3-2 Torque based model along a single Cartesian degree of freedom.....	25
Figure 4-1 Schilling Titan II robot configuration.....	34
Figure 4-2 Robot-environment force/position coordinate system.....	35
Figure 4-3 Input command to the system.....	40
Figure 4-4 Input command to the system-First two seconds.....	41
Figure 4-5 Overall system response: both free fall and contact phase.....	42
Figure 4-6 System response free fall in the Z direction.....	43
Figure 4-7 System response during the contact phase in the X direction.....	44
Figure 4-8 Interaction forces during contact.....	45
Figure 4-9 Forces in the Z direction after contact.....	46
Figure 4-10 Overall forces in the Y direction.....	47
Figure 4-11 Overall torques in the pitch DOF.....	48
Figure 4-12 Overall torques in the roll DOF.....	49
Figure 4-13 Overall torques in the Yaw DOF.....	50

# Acronyms

B	Damping matrix
$B_m$	Joint feedback gains
$b_m$	Invariant joint dynamic parameters
$C(q, \dot{q})$	Centrifugal and Coriolis torque in manipulator frame
$C(x, \dot{x})$	Coriolis and centripetal matrix
D	Arbitrary, positive definite diagonal matrix
DOF	Degree of freedom
DOFs	Degrees of freedom
F	Vector of forces and torques on the manipulator
FMA	Force/moment accommodation
$F_c$	Force and torque commands
$F_e$	Interaction force between environment and end effector
G	Vector of gravity torques
$g(q)$	Gravitational torque in manipulator frame
$g_x(x)$	General gravity forces
$H(q)$	Inertia matrix in manipulator frame
$H_x(x)$	Inertia matrix
HZ	Hertz
$I_r$	Target impedance of the robot
$I_e$	Environment impedance
$J_\theta$	Joint Jacobian matrix

$j\omega$ -axis	Imaginary axis
$K$	Stiffness matrix
$K_e$	Combined stiffness in end effector, grasp, and object
$K_m$	Joint feedback gains
$k_m$	Invariant joint dynamic parameters
$L$	Forward kinematic transformation
$L(\theta)$	Forward kinematic operator
$M$	Mass matrix
$m$	Positive scalar
$m_c$	Invariant joint dynamic parameters
$P$	Vector of all unknown parameters in robot dynamic equation
$S$	Vector of Coriolis, centripetal, and damping torque
TIRT	Target impedance reference trajectory
$W$	Mobility tensor
$X$	Actual trajectory manipulator position
$X_a$	Position adjustment vector
$X_c$	Overall position command
$X_e$	Impedance center of the environment
$X_o$	Nominal trajectory command
$X_v$	Virtual trajectory
$X, \dot{X}, \ddot{X}$	Linear and angular motions of the end effector
$\alpha$	Ratio of $I_r / I_e$

$\theta$	Vector of joint angles
$\tau$	Vector of torques on the joints
$\tau_a$	Vector of adjustment joint torques
$\omega$	Frequency domain
$\Gamma$	Vector of gravity torques in joint model
$\Lambda$	Inertia matrix in joint model
$\Pi$	Vector of Coriolis, centripetal, and damping torque in joint model
$\gg$	Much greater than
( )	Equation number
[ ]	Reference number

# Chapter 1

## Introduction

### 1.1 Introduction and Background

Understanding movement and manipulation and how they may be controlled is the foremost endeavor in robotic field. A control strategy is incorporated in every mechanical manipulator system. There are many concerns associated with robot interaction, concerns such as identifying important features of the environment, making strategic decisions, sensing, selecting, and implementing the appropriate impedance for a given task, stability, etc. Some problems have a distinct artificial intelligence flavor, such as identifying the features of the environment. Others are of a more dynamic nature such as selecting and implementing of an appropriate impedance. Any task that pushes the capabilities of a robot will have aspects of both types of concerns [1].

Robot manipulation may be categorized into two different classes; the first one involves unconstrained motion in space, whereas the second class involves motion that is constrained in some sense by contact with the environment which is external to the robot

manipulator [2]. The first class of manipulation has been subject to extensive research and applications over the past two decades [26]. The second class, while equally important, has been addressed only by a relatively few researchers. The number of applications and amount of experimental work carried out in the second class of manipulation has been correspondingly smaller [3].

The subject of controlling the mechanical interaction between a manipulator and its environment has been addressed by many researchers. The inadequacies of the conventional position and force control are widely recognized and the alternatives are also inadequate. Several control schemes have been proposed such as force control [14,21,22], position control [12], hybrid control [5,11,13], stiffness control [37] and impedance control [1,2,3,4] among others. The impedance control of Hogan [4] provides a unified approach to unconstrained motion control, obstacle avoidance, and constrained manipulation [4].

The work presented in this thesis is an attempt to define different approaches to impedance control, briefly compare the two well-known impedance control techniques (force based and position based) with each other, and design a controller to implement the manipulator variables. Finally, it is the purpose of this thesis to test the theory on a robotic system.

## 1.2 Preview and Outline of the Following Chapters

In chapter 2, previous research and investigation on impedance control, manipulator modeling, and control techniques are presented. Chapter 3 is dedicated to derivation and



modeling of the robot manipulator using both impedance control approaches, environment dynamics, and their relation to each other. Chapter 4 focuses on design of the controller to implement and relate the robot manipulator to the environment dynamics. In chapter 5, the experimental results are presented. Chapter 6 concludes this work and future work and ideas to expand this thesis are discussed.

### 1.3 Terminology and Notations

**TIRT:** The Target Impedance Reference Trajectory concept characterizes the desired dynamic relation of the end effector with the environment. It is usually a differentiable vector function which solves the target impedance dynamics equation in the form of:

$$\mathbf{M}(\ddot{x} - \ddot{x}_v) + \mathbf{B}(\dot{x} - \dot{x}_v) + \mathbf{K}(x - x_v) = -\mathbf{f}_{ext} \quad (1.1)$$

**World frame of reference:** The position of the manipulator will be defined as the position and orientation of its end effector or gripper with respect to a reference frame usually attached to the base of the manipulator. The term "world frame of reference" will be used to define this frame to which the gripper is referenced.

**Task frame of reference:** It is the coordinate frame at the contact point on the object.

**Manipulator frame of reference:** It is the coordinate frame at the contact point on the manipulator.

**Impedance control:** Typically refers to a control law that implements some target dynamics consisting of selected inertial, damping, and stiffness parameters.

# Chapter 2

## Literature Review

### 2.1 Introduction

This section is focused on describing the previous research into that second class of robot manipulation (mentioned in chapter 1) in which robot is constrained by some environmental contacts.

Many robotic tasks, such as those in assembly and machining operations, require the end effector of the robot to establish and maintain contact with the environment. For successful execution of such tasks, both the contact force and the position of the end effector tangent to the contact surface must be simultaneously controlled. This type of "dual control" has been labeled as hybrid control as a matter of consensus in the literature [6,10,20]. This is an appropriate term since the control system must be made of two distinctly different parts while exhibiting the properties of both in a highly blended fashion[5]. In this approach [11], Cartesian axes are separated into those under position

control and those under force control. The robot workspace is divided into orthogonal directions that are constrained either in force or position. Then a force or position controller as appropriate for each direction is built.

Other schemes [4,12] consider the relation between the position and force along each axis. Those axes with large stiffnesses are primarily "position controlled," since force errors are tolerated more than errors in position. Conversely "force controlled" axes have small or zero stiffnesses [4,31,33]. In addition to static behavior, the dynamic interaction between manipulator and environment must also be considered [14,15]. This leads to another strategy, termed impedance control [4], that is based on controlling the relationship between the force applied to the robot manipulator and the position of the manipulator [3].

## 2.2 Hybrid Position/Force Control

As mentioned, prior work on robot control has been dominated by position motion considerations, at both the planning and execution levels. It is assumed that the robot's task may be planned and defined in terms of a series of desired or target motions. The execution or implementation is then to perform these motions with a minimum of error and usually as fast as possible, given the limitations of the hardware. This approach is eminently reasonable and quite successful for non-contact tasks such as arc welding or spray painting, in which the only aspect of the robot's behavior which needs to be controlled is its motion. Prior approaches have also been built based on this motion control strategy, but they have been less successful.

In general, an ideal kinematic constraint divides the workspace of an end effector

into two mutually exclusive subspaces, one in which no motion is possible but force may be exerted, and another in which no force may be exerted but motion is possible. In this way, a contact task may be translated into two dual geometry problems and the desired force in the constrained directions can be planned and defined in a manner exactly analogous to the motions in the unconstrained directions. Motion control is also at the heart of prior approaches to the execution or implementation of contact tasks. Typically, the robot is designed with a fast (frequently analog) motion control servomechanism for each joint. A force control feedback loop (usually digital and slower) is then designed around this motion controller to generate corrections to the commanded motions so as to regulate the force. Unfortunately, this architecture results in problems with contact instability [8].

One drawback associated with most of the earlier works on hybrid control is that they require exact knowledge of the robot dynamic and its interaction with the environment. This is an impractical requirement as in many applications the robot parameters (e.g., payload mass) or the contact surface characteristics may be unknown or vary during the course of the task [5].

Figure 2-1 shows a typical block diagram of a hybrid force/position control system. According to some researchers [4, 20], the impedance control is an enhanced and more realistic (closer to human body behavior than previous methods by considering the environment as a contributing factor to the robot performance) version of hybrid force/position control. As it is described in the following section and chapters, force, position, and the environment characteristic, mainly the environment stiffness and damping, are accounted for as important robot performance parameters.

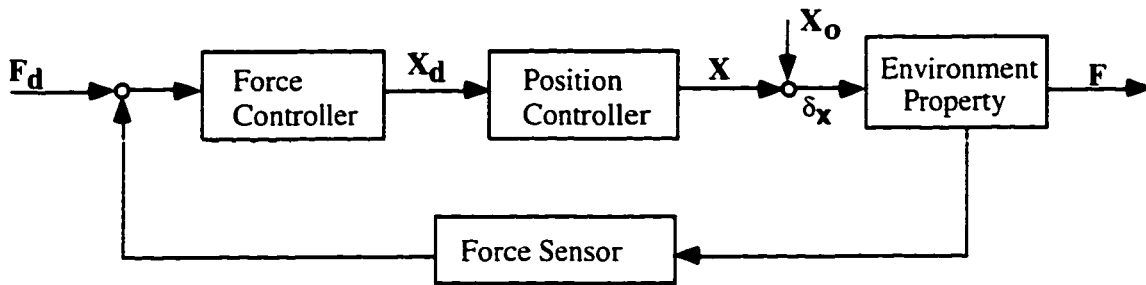


Figure 2-1: Block diagram of one-dimensional force control system

## 2.3 Impedance Control

An alternative to the above approach is to recognize that the dynamic interactions are not a source of disturbances to be rejected, but an integral part of the task. This is the idea behind the impedance control. In impedance control it is assumed that the robot's task must fundamentally be described, not in terms of forces, nor motions, but in terms of the relations between them. In the case of a robot performing contact tasks, that relation should be an impedance. Accordingly, in implementation, the controller is to modulate and regulate not the robot's motion, nor the force it exerts, but its output impedance. In fact, the interaction between a robot and its environment is what any feedback controller really does. The control algorithm implements a relation between sensed quantities and the actuator's efforts. Combined with the hardware, this produces a change in the robot's total dynamic behavior. This change shows up as a modified output impedance at the robot end effector. Therefore, it makes sense to design a controller to do what it naturally does, modify the robot's output impedance [16,17,18].

The term impedance control typically refers to a control law that implements some target dynamics consisting of selected inertia, damping, and stiffness parameters. For example, Kazerooni [2,16] proposes a control law that implements the target dynamic of a generalized n-dimensional damped linear spring on a n-DOF manipulator. Colgate and Hogan [17] propose a control methodology for implementing a generalized single DOF impedance controller. Anderson and Spong [18] propose an inverse dynamic controller that implements a second order linear target dynamics [3,4]. In Stiffness control Cutkuskys and Kao [37] proposed forward and inverse approach of computing the stiffness matrix for control of robotic hands. Li and Kao [38] studied conservative and non-conservative properties of stiffness matrix with gradient and curl vector fields.

Impedance control compares favorably with other similar approaches such as hybrid force/position control, stiffness control, etc. A hybrid combination of motion control and force control in orthogonal directions has been explored. However, hybrid scheme simply combines the motion control and force control approaches and does not circumvent the problems inherent in each. In comparison with others schemes such as stiffness control, impedance control exhibits better performance. That is because the objective of stiffness approach is to implement a relation between force and motion, which is closely related to impedance control. However, stiffness is merely the static component of a robot output impedance. Impedance control goes further and attempts to modulate the dynamics of the robot's interactive behavior [19].

# Chapter 3

## Impedance Control Approaches

### 3.1 Introduction

Impedance control was first proposed by Hogan [4]. The fundamental idea underlying the impedance control is that environmental constraints impose a relationship between the position of the manipulator and the contact force exerted by the environment. Hogan points out that this relationship can be modeled by a generalized nonlinear impedance, consisting of some inertia, damping, and stiffness characteristic that describe the relationship. Consequently, Hogan hypothesizes that a viable control strategy for the contact tasks would be to give the manipulator an impedance complimentary to that of the environment. The combined manipulator and environment system should then be well behaved, much like a matched impedance electrical circuit [20]. In other words, a certain desired dynamic specification of manipulator behavior, the manipulator impedance, is considered. Impedance describes the dynamic relation between positions (and orientation) and forces (and torques). There are two common approaches in providing this impedance

via feedback control, in an idealized sense, generally referred to as position based and torque based approaches [7].

## 3.2 Preliminaries

Let us consider the following relationship between effort and motion about a nominal end effector trajectory point  $X_0$ :

$$\mathbf{f} = \mathbf{M}(\ddot{\mathbf{x}} - \ddot{\mathbf{x}}_o) + \mathbf{B}(\dot{\mathbf{x}} - \dot{\mathbf{x}}_o) + \mathbf{K}(\mathbf{x} - \mathbf{x}_o) \quad (3.1)$$

where  $\mathbf{F}$  is a vector of forces and torques on the manipulator due to contact with the environment, and  $\mathbf{X}$ ,  $\dot{\mathbf{x}}$ , and  $\ddot{\mathbf{x}}$  represent the linear and angular motions of the end effector. Since  $\mathbf{F}$  is identically zero if and only if  $(\mathbf{X} - \mathbf{X}_0)$  is identically zero, the trajectory  $\mathbf{X}_0$  is interpreted as the non-contact end effector trajectory. As the end effector is perturbed by an external force  $\mathbf{f}$ , equation (3.1) describes the dynamics of the trajectory perturbation  $(\mathbf{X} - \mathbf{X}_0)$ .

The impedance specified by (3.1) is given in the frequency domain by the following matrix:

$$\mathbf{Z} = \left[ \mathbf{f}_i / \left( x_j - x_{o,j} \right) \right] = \mathbf{M}s^2 + \mathbf{B}s + \mathbf{K} \quad (3.2)$$

The parameter  $\mathbf{K}$  is the stiffness matrix,  $\mathbf{B}$  is the damping matrix, and  $\mathbf{M}$  is the mass matrix. These parameters can be selected to correspond to various manipulation task objectives.



Typically high stiffness is specified in directions where the environment is compliant and positioning accuracy is important. Low stiffness is specified in directions where the environment is stiff or when small interaction forces must be maintained. Large damping values are specified when energy must be dissipated, and inertia values can be used to provide smoothness in the end effector response due to external contact. The form of equation (3.2) suggests that the parameter matrices  $\mathbf{K}$ ,  $\mathbf{B}$ , and  $\mathbf{M}$  need not be diagonal. For particular tasks, coupling between impedance axes may be useful but only uncoupled impedances are considered here, i.e. diagonal  $\mathbf{K}$ ,  $\mathbf{B}$ , and  $\mathbf{M}$  [12,22,23].

The manipulator is controlled to provide the above impedance specifications by treating the mechanism either as an actuator of position or an actuator of force and torque. For the position based approach, forces and torques are sensed explicitly, e.g. via a wrist force/torque sensor, and position commands are issued to the inner loop controller. In particular, the position adjustment vector  $\mathbf{X}_a$  is created by filtering the measured interaction forces and torques  $\mathbf{f}$  to satisfy:

$$\mathbf{f} = \mathbf{M}\ddot{\mathbf{x}}_a + \mathbf{B}\dot{\mathbf{x}}_a + \mathbf{K}\mathbf{x}_a \quad (3.3)$$

via

$$\mathbf{x}_a(s) = \left[ \mathbf{M}s^2 + \mathbf{B}s + \mathbf{K} \right]^{-1} \mathbf{F}(s) \quad (3.4)$$

With the simplification of diagonal  $\mathbf{K}$ ,  $\mathbf{B}$ , and  $\mathbf{M}$ , this reduces to a second order low pass filter for each component of  $\mathbf{f}$  to generate the respective components of  $\mathbf{X}_a$  [12,22].

The adjustment  $\mathbf{X}_a$  is added to the nominal trajectory command  $\mathbf{X}_O$  to generate the overall position command  $\mathbf{X}_C$ :

$$x_c = x_o + x_a \quad (3.5)$$

Note that when  $F \equiv 0$  (no environmental contact) then  $x_c = x_o$ . If the manipulator has the ability to accurately enforce this command, i.e.

$$x \equiv x_c \quad \text{then} \quad x_a = x - x_o \quad (3.6)$$

and the control laws (3.4) and (3.5) satisfy the original impedance specification (3.1). Thus, the position based impedance control approach relies on accurate position control of the manipulator inside the actual impedance control loop [12,14,23].

In the torque based impedance control approach [4,21], positions are sensed, and force and torque commands  $f_c$  (the forces and torques on the environment) are computed from the nominal trajectory  $X_o$  and the actual trajectory  $X$  via :

$$f_c = \mathbf{M}(\ddot{x}_o - \ddot{x}) + \mathbf{B}(\dot{x}_o - \dot{x}) + \mathbf{K}(x_o - x) \quad (3.7)$$

Clearly, if the manipulator can accurately supply these forces at the end effector via joint torques such that  $f_c \equiv -f$ , then the control law (3.7) provides the impedance specified in (3.1). This approach relies on the manipulator as an actuator of force and torque, which may also require an inner loop control in addition to the impedance control loop. Note that a force sensor is not explicitly required in the torque based approach [12,14].

As a practical matter, any manipulator can not be controlled to be a perfect position or force source. An impedance control implementation will therefore be an inaccurate way to provide desired impedances at best, and may provide unacceptable behavior in some cases [23]. The bulk of this thesis is concerned with quantifying the behavior of these two fundamental approaches.

### **3.2.1 Position Based Impedance Control**

This form of impedance control relies on accurate position control of the manipulator as a basis. The impedance control is added as an additional control loop around the position controlled manipulator. This basis makes it an attractive approach for typical industrial manipulators, since they are often designed as accurate (or at least repeatable) positioning devices. More specifically, they are often very stiff structurally and therefore are comparatively heavy. For electric manipulators the large gravity loads usually imply significant gear reduction at the actuators to maintain reasonable power dissipation and joint position or rate control to improve operational safety [7,12].

First, a representative dynamic model of this class of manipulators is considered. This model will be derived based on a full dynamic representation but simplified according to the following assumptions:

- High gain joint position control is in effect.
- Gear ratios at the joint actuators are large.

Time delays in the impedance control loop can often be significant because it is a Cartesian control loop, and transformations between joint space and Cartesian space are necessary to provide proper joint actuator commands. Moreover, transformations between

various Cartesian coordinate frames can also be required. However, for the purposes of this thesis and sake of simplicity, time delays and their effects are not discussed here [7,12,23].

Impedance specifications are often most naturally expressed in terms of the task coordinate frame, since the task geometry determines which directions are motion constrained or force sensitive. Thus, the impedance specification filter (3.4) would be in terms of task coordinates. However, the kinematic transformations of the manipulator may be provided in terms of the fixed world frame, fixed at the base of the manipulator since nominal Cartesian motion commands are often in terms of this world frame. The impedance control loop would therefore consist of the filter equation (3.4) followed by a coordinate frame change, followed by equation (3.5), followed by the inverse kinematic transformation to arrive at the joint position commands. Note that in order to compute the coordinate frame change between task and world frame, the position of the task relative to the manipulator base frame must be computed typically via the forward kinematic transformation. A final source of difficulty is the treatment of orientations in the impedance control loop. Depending on the specific orientation representation, e.g. Euler angles, direction cosines, quaternions, etc., the combination of orientation updates in  $X_a$  with the nominal commands  $X_c$  is more complicated than a simple sum. These updates can contribute to the overall time delay in the impedance control loop [7,12,13].

Our model of the position controlled manipulator begins with the Euler-Lagrange formulation of:

$$\tau_a = \mathbf{M}(\theta)\ddot{\theta} + \mathbf{S}(\theta, \dot{\theta}) + \mathbf{G}(\theta) + \tau \quad (3.8)$$

where  $\tau_a$  is the vector of joint torques supplied by the joint actuators,  $\theta$  is the vector of joint angles, and  $\tau$  is the vector of torques on the joints due to contact with the environment at the end effector.  $M(\theta)$  is the inertia matrix of the joint space,  $S$  is the vector of Coriolis, centripetal, and damping torque, and  $G$  is the vector of gravity torques [12,21,23].

In Cartesian coordinates, this model has the following form:

$$\mathbf{f}_a = \Lambda(X)\ddot{X} + \Pi(X, \dot{X}) + \Gamma(X) - \mathbf{f} \quad (3.9)$$

Using the forward kinematic transformation  $L$ , where  $X = L(\theta)$ , and the corresponding Jacobean  $J(\theta)$ , this model relates to the joint model via

$$\mathbf{f}_a = \mathbf{J}^{-T}(\theta)\tau_a \quad \text{and} \quad \mathbf{f} = \mathbf{J}^{-T}(\theta)\tau \quad (3.10)$$

$\Lambda$ ,  $\Pi$ , and  $\Gamma$  correspond to  $M$ ,  $S$ , and  $G$  in (3.8). This correspondence is given in details in [3,12,21,23].

The joint position control law considered to be in form of:

$$\tau_a = \mathbf{K}_m(\theta_r - \theta) - \mathbf{B}_m\dot{\theta} \quad (3.11)$$

which has the Cartesian form of:

$$\begin{aligned} \mathbf{f}_a = \mathbf{J}^{-T}(\theta) \left[ \mathbf{K}_m (\theta_r - \theta) - \mathbf{B}_m \dot{\theta} \right] = \mathbf{J}^{-T}(\theta) \mathbf{K}_m \mathbf{L}^{-1}(x_c) \\ - \mathbf{J}^{-T}(\theta) \mathbf{K}_m \mathbf{L}^{-1}(x) - \mathbf{J}^{-T}(\theta) \mathbf{B}_m \mathbf{J}^{-1}(\theta) \dot{x} \end{aligned} \quad (3.12)$$

Next step is to model the behavior of the manipulator under impedance control in the neighborhood of the contact point where environmental interaction takes place. That is, it is assumed the actual manipulator position  $\mathbf{X}$  is near the commanded position  $\mathbf{X}_c$ . It is also assumed that this contact point in joint coordinates is well away from any kinematic singularities. Thus, we use the approximation:

$$\mathbf{L}^{-1}(x_c) - \mathbf{L}^{-1}(x) \approx \mathbf{J}^{-1}(\theta)(x_c - x) \quad (3.13)$$

obtained from a Taylor series expansion of  $\mathbf{L}^{-1}$  about  $\mathbf{X}_c$ . Using this approximation in equation (3.12), and equating it with equation (3.9) yields the Cartesian representation of the closed loop manipulator dynamics:

$$\begin{aligned} \mathbf{J}^{-T}(\theta) \mathbf{K}_m \mathbf{J}^{-1}(\theta) x_c = \Lambda(x) \ddot{x} + \Pi(x, \dot{x}) + \Gamma(x) \\ + \mathbf{J}^{-T}(\theta) \mathbf{B}_m \mathbf{J}^{-1}(\theta) \dot{x} + \mathbf{J}^{-T}(\theta) \mathbf{K}_m \mathbf{J}^{-T}(\theta) x - \mathbf{f} \end{aligned} \quad (3.14)$$

Now when the external force  $\mathbf{f}$  is zero, or supplied by a pure force source (zero source impedance), the dynamics of the position controlled manipulator are unchanged. In control terminology, the natural response of the system is unchanged and  $\mathbf{f}$  can be considered an additional input which affects the forced response along with  $\mathbf{X}_c$ . Thus, the stability properties of the system are also unchanged [7,12,21,23].

However, when the external force depends on the manipulator position, then the presence of  $f$  in equation (3.14) represents an additional feedback loop; dynamics and stability can be affected [15]. This relation is considered between  $f$  and  $X$  (the environmental impedance) at the contact point to be dominated by a stiffness, i.e.

$$\mathbf{f} = \mathbf{K}_e (x_e - x_a) \quad (3.15)$$

where  $X_e$  is the impedance center of the environment, and the stiffness  $K_e$  represents the combined stiffness in the end effector, grasp, and object in both position and orientation (recall  $F$  is the force and torque on the manipulator by the environment.). This would represent the case where the manipulator has securely grasped a fixed object. It is also assumed  $X_e = X_o$ , which is the case where the manipulator grasp is in the nominally "relaxed" state where the interaction force is zero. Examining the equation (3.5) implies that  $X_c$  is nominally equal to  $X_o$ . These simplifying assumptions reduce the accuracy of the model in general manipulator motion and environmental interaction. However, satisfactory behavior, in this situation where environmental interaction is small, is a necessary condition for smooth and stable interaction in general [3,12,13,23,26].

For  $X$  in the neighborhood of  $X_c$  and  $X_o$  the nonlinear model of equation (3.14) is approximated arbitrarily and closely by the linear model:

$$\begin{aligned} \mathbf{J}_c^{-T} \mathbf{K}_m \mathbf{J}_c^{-1} x_c + \mathbf{K}_e x_o &= \Lambda(x_c) \ddot{x} + \Pi(x, \dot{x}) + \Gamma(x) \\ + \mathbf{J}_c^{-T} \mathbf{B}_m \mathbf{J}_c^{-1} \dot{x} + \mathbf{J}_c^{-T} \mathbf{K}_m \mathbf{J}_c^{-1} x + \mathbf{K}_e x & \end{aligned} \quad (3.16)$$

where  $J_c = J(\theta_c)$  and  $\theta_c$  corresponds to  $X_c$ , i.e.  $\theta_c = L^{-1}(X_c)$ .

Typically, the joint feedback gains  $K_m$  and  $B_m$  are quite large. This provides the disturbance rejection necessary to achieve accurate position control. It also allows further simplification of the closed loop dynamics. In particular, we assume that:

- $J_c^{-T} K_m J_c^{-1} \gg \Gamma(x)$  (in the vector norm sense)
- $J_c^{-T} K_m J_c^{-1} \gg K_e$  (in the positive definite, matrix sense)
- $J_c^{-T} B_m J_c^{-1} \dot{x} \gg \Pi(x, \dot{x})$  (in the vector norm sense)

Using the following relationship:

$$\Lambda(x) = J^{-T}(\theta) M(\theta) J^{-1}(\theta) \quad (3.17)$$

along with the above assumptions, we obtain the simplified closed loop manipulator dynamics:

$$J_c^{-T} [K_m] J_c^{-1} x_c = J_c^{-T} [M(\theta_c) s^2 + B_m s + K_m] J_c^{-1} x \quad (3.18)$$

in the frequency domain. Again, this should be interpreted as a "small signal" model since it holds only for  $X$  in the neighborhood of  $X_c$  and  $X_0$  [21,24,25].

This simplified model shows that the Cartesian dynamics are determined by  $M(\theta_c)$ ,  $B_m$ , and  $K_m$  except for a change of basis given by  $J_c^{-1}$ . Actually,  $K_m$  and  $B_m$  are



diagonal by design (independent joint control) and  $M(\theta_c)$  is often diagonally dominant due to the large gear ratios at the actuators. This combination allows for an even more straight forward interpretation of (3.18). Specifically, suppose that these matrices have the same structure, i.e.

$$\mathbf{M}(\theta_c) = m_c \mathbf{D} \quad (3.19)$$

$$\mathbf{B}_m = b_m \mathbf{D}$$

$$\mathbf{K}_m = k_m \mathbf{D}$$

where  $D$  is an arbitrary positive definite diagonal matrix. This assumption means that the joint controllers are tuned to give the same joint dynamics for all joints, i.e. the same bandwidth and damping ratios. Since the joint moments of inertia vary considerably from joint to joint, the joint position and rate gains must also vary. Hence, the joint stiffnesses and dampings are not the same for all joints. The entries of  $D$  reflect this scaling of joint impedances, while the scalars  $m_c$ ,  $b_m$ , and  $k_m$  parameterize the invariant joint dynamic behavior [31,15,17].

Substituting equations (3.19) into equation (3.18) yields:

$$\mathbf{J}_c^{-T} \mathbf{D} \mathbf{J}_c^{-1} k_m x_c = \mathbf{J}_c^{-T} \mathbf{D} \mathbf{J}_c^{-1} \left[ m_c s^2 + b_m s + k_m \right] x \quad (3.20)$$

Since  $\mathbf{J}_c^{-T} \mathbf{D} \mathbf{J}_c^{-1}$  is invertible, we obtain the diagonal or decoupled system:

$$k_m x_c = [m_c s^2 + b_m s + k_m] x \quad (3.21)$$

in which every Cartesian DOF has the same simple dynamic model. This is the model used to examine the stability of the position based impedance control approach. The intent is to understand the first order or most significant properties of impedance control.

The impedance control loop given by equations (3.4) and (3.5) is also assumed to be decoupled; hence, for any particular Cartesian axis, there is the following set of scalar equations modeling the behavior of the overall system:

$$k_m x_c = [m_c s^2 + b_m s + k_m] x \quad (3.22)$$

$$x_a = [j s^2 + b s + k] f$$

$$f = e^{-s T_d} k_e (x_e - x)$$

$$x_e = x_o + x_a$$

Recall that  $f$  is the sensed interaction force. Note that a time delay of  $T_d$  second is included in the impedance control loop to account for computation delays. This is shown in the block diagram in Figure 3-1. A stability analysis of this system has been performed under various assumptions in [12,23,25].

The open loop transfer function of the model in equation (3.22) is:

$$\frac{x_a}{x_c} = -\frac{k_m k_e e^{-sT_d}}{(m_c s^2 + b_m s + k_m)(js^2 + bs + k)} \quad (3.23)$$

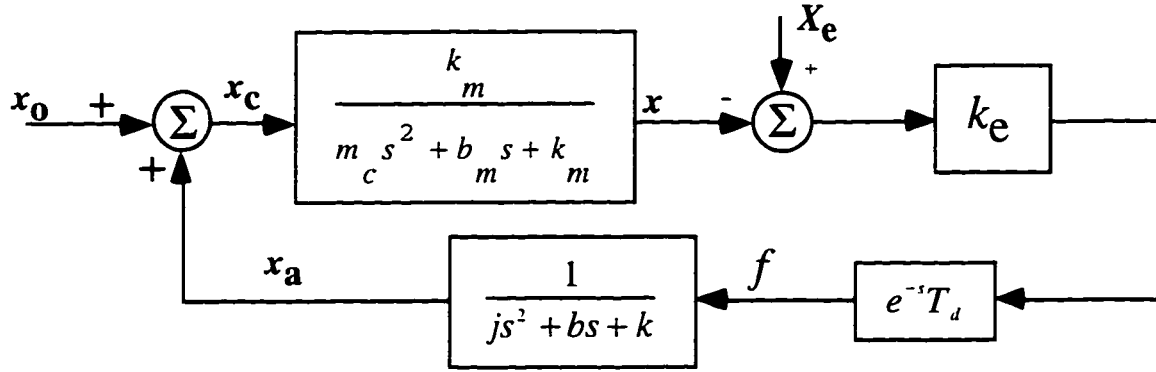


Figure 3-1 Position based model along a Cartesian single degree of freedom

Provided that the damping ratios of the manipulator dynamics and the impedance filter are larger than  $\sqrt{2} / 2$ , the stability of the system depends only on a positive phase margin [7]. Setting the phase margin equal to zero provides a relation between the impedance control design parameters  $k$ ,  $b$ , and  $j$  which yields a marginally stable closed loop system.

This relation is given by the two non linear equations in the frequency domain  $\omega$ :

$$k_m k_e = \sqrt{[(k_m - \omega^2 m_c)^2 + b_m^2 \omega^2][(k - \omega^2 j)^2 + b^2 \omega^2]} \quad (3.24)$$

$$\pi = -\tan^{-1}\left(\frac{b_m \omega}{k_m - \omega^2 m_c}\right) - \tan^{-1}\left(\frac{b \omega}{k - \omega^2 j}\right) - \omega t_d$$

which can be solved numerically for any particular parameters. Reference [7] has the stability boundaries of the impedance control system (solutions of equation (3.24)) for parameters obtained from an industrial manipulator for various time delays ( $T_d$ ) [7,12,18,23].

### **3.2.2 Torque Based Impedance Control**

In the torque based approach, positions are measured and force commands are computed to satisfy the impedance objectives. Since direct sensing of Cartesian positions and orientations is usually not practical, Cartesian positions must be computed via kinematic transformations and measured joint angles. Cartesian velocities and accelerations can be directly measured more easily, although this information can also be derived from joint measurements. In either case, there is often significant time delay in computing or measuring these quantities. As in the position based approach, representation of orientations and transformation from one reference frame to another can also add to the computations necessary in implementing impedance control. Finally, the Cartesian force and torque commands must be transformed into joint coordinates, using the kinematic jacobian to obtain the actuator torque commands. In this section, the torque based impedance control is modeled, developed, and compared with the similar conditions in position based approach. First, a dynamic model of the overall impedance control system will be developed. This model will be analyzed along one Cartesian DOF to determine its stability boundaries [21,24].

We begin with the manipulator model in Cartesian coordinates:

$$\mathbf{f}_a = \Lambda(x)\ddot{x} + \Pi(x, \dot{x}) + \Gamma(x) - \mathbf{f} \quad (3.25)$$

as in equation (3.9). Since the dynamics represented by  $\Lambda$ ,  $\Pi$ , and  $\Gamma$  detract from the actuator torque, the torque and force  $\mathbf{f}$  will not be equal to  $-\mathbf{f}_a$ . The following inner loop torque compensation is often suggested [4,21,26] to simplify these dynamic effects:

$$\mathbf{f}_a = \frac{1}{m} \Lambda(x) + \Pi(x, \dot{x}) + \Gamma(x) - \mathbf{f} \quad (3.26)$$

where  $m$  is a positive scalar and  $\mathbf{f}_c$  is the new command vector. The vector  $\mathbf{f}$  is obtained by measuring the interaction force directly via a force sensor. This is only used to provide decoupling in the system dynamics and would not be necessary otherwise. Equating equations (3.26) and (3.25) results in the following closed loop dynamic model:

$$\mathbf{f}_c = m\ddot{x} \quad (3.27)$$

Similar to the case in section 3.2.1, the source impedance of the external force  $\mathbf{f}$  does not affect the system dynamics. In the position based approach, large joint control gains "swamp out" the effect of this environmental impedance; in the torque based case, the environmental impedance effect is "canceled out" using force measurements [24,31].

As in section 3.2.1 the Cartesian force and torque command  $\mathbf{f}_c$  is computed to satisfy the desired impedance specification, but is delayed  $T_d$  seconds due to computation delays. Thus, the impedance control loop is described by:

$$\mathbf{f}_c = e^{-sT_d} [\mathbf{J}s^2 + \mathbf{B}s + \mathbf{K}](x_o - x) \quad (3.28)$$

If we use the fact that K, B, and J are diagonal, then the open loop transfer function of the impedance control system along any particular Cartesian DOF becomes:

$$\frac{x}{x_c} = - \frac{(js^2 + bs + k)e^{-sT_d}}{ms^2} \quad (3.29)$$

This model is shown in block diagram of Figure 3-2 [21,26].

Since the open loop magnitude function is monotone (decreasing), this system is marginally stable when k, b, j, and the frequency  $\omega$  satisfy the magnitude and phase conditions:

$$m\omega^2 = \sqrt{(k - j\omega^2)^2 + b^2\omega^2} \quad (3.30)$$

$$0 = -\tan^{-1}\left(\frac{b\omega}{k - j\omega^2}\right) - \omega T_d$$

Thus, these equations provide the stability boundary in the specified impedance parameters k, b, and j for various time delays  $T_d$ . The above set of nonlinear equations can be solved numerically for a particular j to determine the relation between k and b for overall system stability. Reference [7] has the graphical representations of these boundaries for particular manipulator parameters:  $j=0$  and various time delays.

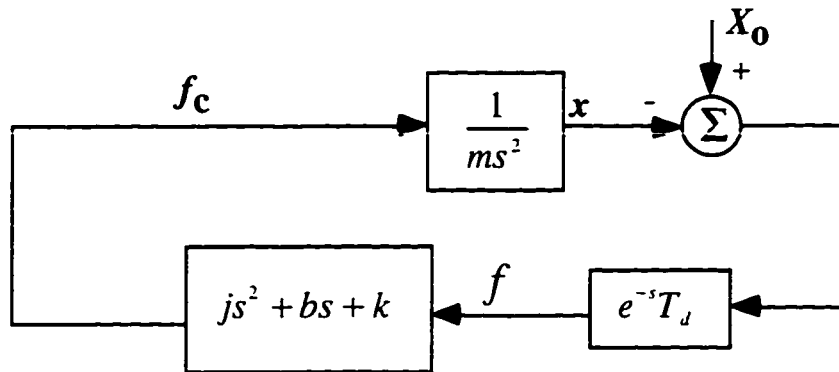


Figure 3-2 Torque based model along a single Cartesian degree of freedom

### 3.3 Summary

In an ideal sense, impedance control can be implemented in more than one way. Two approaches were examined here, the position and torque based methods. When implementation effects are considered, these two schemes perform quite differently. Using a similar manipulator model and similar values of computation time delays, these approaches have shown to have the following general properties [7,24].

The position based approach suffers from an inability to provide very "soft" impedances, i.e. small stiffness and damping. This approach would be generally desirable in cases where stiff joint position control is required for other reasons, e.g. it is already present, to improve safety should outer control loops fail, or in cases where high accuracy positioning is required in some Cartesian directions. Although this approach requires a force sensor, interaction forces are directly sensed and effectively filtered by the impedance control loop. Thus, noise problems are not aggravated [24].

The analysis of Section 3.2.1 supports the control-theoretic notion that large feedback gains (small  $k$  and  $b$  in the impedance control loop of equation (3.22)) together with time delays or additional system dynamics often lead to instability [14,15]. The manipulator is "stiffened" by the simple high-rate joint position control loops, then "softened" by the slower and more complex Cartesian impedance loop. The second loop is more limited in its ability to change system behavior; hence, "soft" impedances are more difficult to provide [7,24].

The torque based approach is complimentary in a sense that it is the large stiffnesses that are difficult to provide. However, it is comparatively better suited to provide the small stiffnesses and dampings desired in reducing contact forces [24,31].

The torque based approach is suited to applications where manipulator gravity loads are small and motions are slow, when the complex inner loop (inverse dynamics) control can be provided at sufficiently high rates, or when the required manipulator modeling details are available. Sensing of Cartesian positions and rates are required directly or indirectly via measurement of joint variables. This can intensify problems with signal noise and time delays [23].



# Chapter 4

## Controller Design and Experimental Results

### 4.1 Introduction

In this section an  $n$ -DOF manipulator is modeled along with its target impedance. An impedance control law is designed to implement the system. The overall system is then being tested experimentally using a Schilling Titan II manipulator and the results are presented.

### 4.2 Preliminaries

First let us examine the differences of a constrained motion control from an unconstrained motion control. In constrained motion control one deals with the problem of regulating the mechanical impedance of the robot which involves external force/torque

measurements rather than controlling end effector position/orientation which is independent of environment (unconstrained). As will be shown in section 4.3.2 by introducing the concept of target impedance reference trajectory (TIRT) the desired dynamic relation of the end point with environment is characterized in a manner similar to [27].

## 4.2.1 The Dynamic Models

Dynamics of an n-DOF manipulator can be described by:

$$\mathbf{H}(q)\ddot{q} + \mathbf{C}(q, \dot{q})\dot{q} + \mathbf{g}(q) + \mathbf{f}(\dot{q}) = \boldsymbol{\tau} - \mathbf{J}^T \mathbf{f}_{\text{ext}} \quad (4.1)$$

when controlling the dynamic behavior of the end effector, environment interaction comes to be a main concern. It is often desirable to describe the manipulator dynamics in its operational (i.e. Cartesian) space as [27]:

$$\mathbf{H}_x(x)\ddot{x} + \mathbf{C}_x(x, \dot{x})\dot{x} + \mathbf{g}_x(x) + \mathbf{f}_x(\dot{x}) = \mathbf{J}^T \boldsymbol{\tau} - \mathbf{f}_{\text{ext}} \quad (4.2)$$

where

$$\begin{aligned} \mathbf{H}_x &= \mathbf{J}^T \mathbf{H} \mathbf{J}^{-1}, & \mathbf{C}_x(x, \dot{x}) &= \mathbf{J}^{-T} (\mathbf{C} - \mathbf{H} \mathbf{J}^{-1} \dot{\mathbf{J}}) \mathbf{J}^{-1}, \\ \mathbf{g}_x &= \mathbf{J}^{-T} \mathbf{g}, & \mathbf{f}_x(\dot{x}) &= \mathbf{J}^{-T} \mathbf{f} \end{aligned}$$

## 4.2.2 The Conventional Impedance Control

In impedance control, the target impedance is usually specified as a second order dynamics [8]:

$$\mathbf{M}(\ddot{x} - \ddot{x}_v) + \mathbf{B}(\dot{x} - \dot{x}_v) + \mathbf{K}(x - x_v) = 0 \quad (4.3)$$

where  $X_v$  is the virtual trajectory that often coincides with the desired trajectory when no contact occurs. However, it will most likely correspond to positions beyond the robot workspace during the contact in order to maintain a proper amount of contact, see [28] for more details.

Given manipulator dynamics (4.2) and target impedance (4.3), it is quite natural to use a constrained motion control counterpart of the well known resolved acceleration algorithm [29] to design a control torque  $\tau$  such that the overall system dynamics coincides with that given in (4.3). Such a torque is given by  $\tau = \mathbf{J}^T \mathbf{f}$  with:

$$\mathbf{f} = \mathbf{f}_{\text{ext}} + \mathbf{C}_x \dot{x} + g_x + \mathbf{f}_x + \mathbf{H}_x \left\{ \ddot{x}_v - \mathbf{M}^{-1} [\mathbf{B}(\dot{x} - \dot{x}_v) + \mathbf{K}(x - x_v) + \mathbf{f}_{\text{ext}}] \right\} \quad (4.4)$$

or in the notation of [4],

$$\begin{aligned} \tau = \mathbf{J}^T \{ & \mathbf{W}^{-1} [\mathbf{M}^{-1} (\mathbf{K}(x_v - \mathbf{L}(\theta)) + \mathbf{B}(\dot{x}_v - \mathbf{J}\dot{\theta})) + \ddot{x}_v \\ & + \mathbf{J}\mathbf{H}^{-1} (\mathbf{C}\dot{\theta} + g + f) - j\dot{\theta}] + [\mathbf{I} - \mathbf{W}^{-1}\mathbf{M}^{-1}] \mathbf{f}_{\text{ext}} \} \end{aligned} \quad (4.5)$$

where  $\mathbf{L}(\theta)$  represents the forward kinematics operator which maps a set of joint displacements into the corresponding end point position and orientation, and  $\mathbf{W} = \mathbf{J}\mathbf{H}^{-1}\mathbf{J}^T$  is the mobility tensor [4] whose inverse is the actual inertia of the robot end effector [8]. The control law in equation (4.5) has been known as impedance control for constrained motion of robots where the major control task is to regulate the dynamic relation of the end effector with the environment to be contacted. It follows from the above observation that the

impedance control is indeed a duality of the resolved acceleration control in the domain of constrained motion control [16,29,31].

Note that the introduction of the mobility tensor  $W$  in this case allows us to avoid performing inverse operation for the rectangular Jacobian. However, the control torque expression in (4.5) is certainly not computation efficient when the manipulator has six DOF and its Jacobian is nonsingular. As a matter of fact, it can readily be shown that the control torque  $\tau$  can be computed using the following formula[30]:

$$\tau = \mathbf{H}\ddot{\theta}^* + \mathbf{C}\dot{\theta} + g + f + \mathbf{J}^T \mathbf{f}_{\text{ext}} \quad (4.6)$$

where  $\ddot{\theta}^*$  is given by

$$\ddot{\theta}^* = (\mathbf{M}\mathbf{J})^{-1} \left[ \mathbf{K}(x_v - \mathbf{L}(\theta)) + \mathbf{B}(\dot{x}_v - \mathbf{J}\dot{\theta}) + \mathbf{M}\ddot{x}_v - \mathbf{J}\dot{\theta} - \mathbf{f}_{\text{ext}} \right] \quad (4.7)$$

Therefore, the measurements from the joint position/velocity sensors as well as the wrist force sensor can be used to compute  $\ddot{\theta}^*$  and adopt in turn the recursive Newton-Euler computation scheme to compute the sum of the first four terms on the right hand side of equation (4.6) [8,30].

## 4.3 The Control Algorithm

### 4.3.1 Impedance Control with Estimated Dynamics

The basic idea behind the estimation method is to consider the robot and environment as a whole system. The input and output variables are the desired force  $F_d$

and the interaction force  $F_e$ . Using the relationships between them, we obtain the environment model without measuring its deformation [16,30].

Let  $p \in R^{n_i}$  denote the vector of all unknown parameters in the robot dynamic equation (4.2) and  $\hat{p} \in R^{n_i}$  its estimate from a control law to be specified later. The impedance control can be implemented if the estimated parameter values are used in equation (4.4) or (4.6). For the sake of simplicity, it is assumed that the Jacobian is a square and nonsingular matrix. The control torque can then be written as:

$$\tau = \hat{\mathbf{H}}\ddot{\theta}^* + \hat{\mathbf{C}}\dot{\theta} + \hat{g} + \hat{f} + \mathbf{J}^T \mathbf{f}_{\text{ext}} \quad (4.8)$$

where  $\hat{H}$ ,  $\hat{C}$ ,  $\hat{g}$ , and  $\hat{f}$  are evaluated using estimated parameters. Similar to the discussion in section 4.2.2, the recursive Newton-Euler computation schemes [30] applies to equation (4.8), making it a numerically attractive formulation in implementing the proposed control algorithm [16,29,31].

In order to perform an error analysis, however, it is more convenient to write the control torque as  $\tau = \mathbf{J}^T \mathbf{f}$  with

$$\mathbf{f} = \mathbf{f}_{\text{ext}} + \hat{\mathbf{C}}_x \dot{x} + \hat{g}_x + \hat{f}_x + \hat{\mathbf{H}}_x \left\{ \ddot{x}_v - \mathbf{M}^{-1} \left[ \mathbf{B}(\dot{x} - \dot{x}_v) + \mathbf{K}(x - x_v) + \mathbf{f}_{\text{ext}} \right] \right\} \quad (4.9)$$

Another method is discussed in [31].

### 4.3.2 The Target Impedance Reference trajectory (TIRT)

Given the desired end point environment relation (4.3), the TIRT is a differentiable vector function  $x_r(t)$  of time, which solves the second order differential equation (4.3) with a proper set of initial conditions, e. g.  $x_r(0) = x_v(0)$  and  $\dot{x}_r(0) = \dot{x}_v(0)$ . Clearly, the TIRT as a function of time coincides with the desired tracking trajectory over the unconstrained motion duration simply because  $F_{ext} = 0$ . However, it may differ from the pre-assigned virtual trajectory considerably during the contact. This is particularly true when either the environment involved has a very high stiffness, or the target impedances are assigned such that their dynamics have a pole sufficiently close to the  $j\omega$ -axis. To be specific, the TIRT  $x_r(t)$  is defined as the unique solution of the following initial-value problem [1,27]:

$$\mathbf{M}\ddot{x}_r + \mathbf{B}\dot{x}_r + \mathbf{K}x_r = -\mathbf{f}_{ext} + (\mathbf{M}\ddot{x}_v + \mathbf{B}\dot{x}_v + \mathbf{K}x_v) \quad (4.10)$$

with  $x_r(0) = x_v(0)$ ,  $\dot{x}_r(0) = \dot{x}_v(0)$

A couple of remarks on the concept introduced above are now in order. First, with measurements from the wrist force sensor and the given virtual trajectory, the target impedance reference trajectory can be formed very quickly during each sampling duration by numerically integrating equation (4.10). Furthermore, notice that such numerical integration is necessary only during the contact since one may otherwise simply take  $x_r(t) = x_v(t)$ . Second, the importance of this concept is due to the fact that analytically the essence of impedance control is to perform the dynamic relation for the end point

environment interaction such that the end point motion could follow the TIRT. The importance of equation (4.10) will become apparent when an attempt is made to derive an error equation for end effector position [29,30].

## 4.4 Experimental Results

A 6 DOF planar robot was considered to verify the validity of the proposed algorithm in section 4.2.2. The arm configuration and the environment surface are shown in figure 4-1. The target impedance reference trajectory (damping and stiffness) is implemented in the Z direction. Also, the position control is measured in this direction.

### 4.4.1 Experimental Setup

A task was designed for the purposes of the experiment. The task constitutes the robot moving freely in the air toward a surface at first (in the Z direction), and then after colliding with the surface (environment) sliding along the X direction with a constant force in the Z direction, see figure 4-2. A smooth ball joint roller attached to the robot end effector is used to make the sliding as friction free and smooth as possible. The end point is then required to be in contact with the table while sliding down the path on the environment surface. The actual position of the end effector  $X$  and the input command position  $X_c$  are shown in figure 4-3 and 4-4. In order to have contact stability during the experiment, it was necessary to provide some type of environment that would give consistent results for contact experiment. For the purposes of this thesis, a 1/2-inch steel plate was used as the environment. The steel plate was clamped securely to the table. The

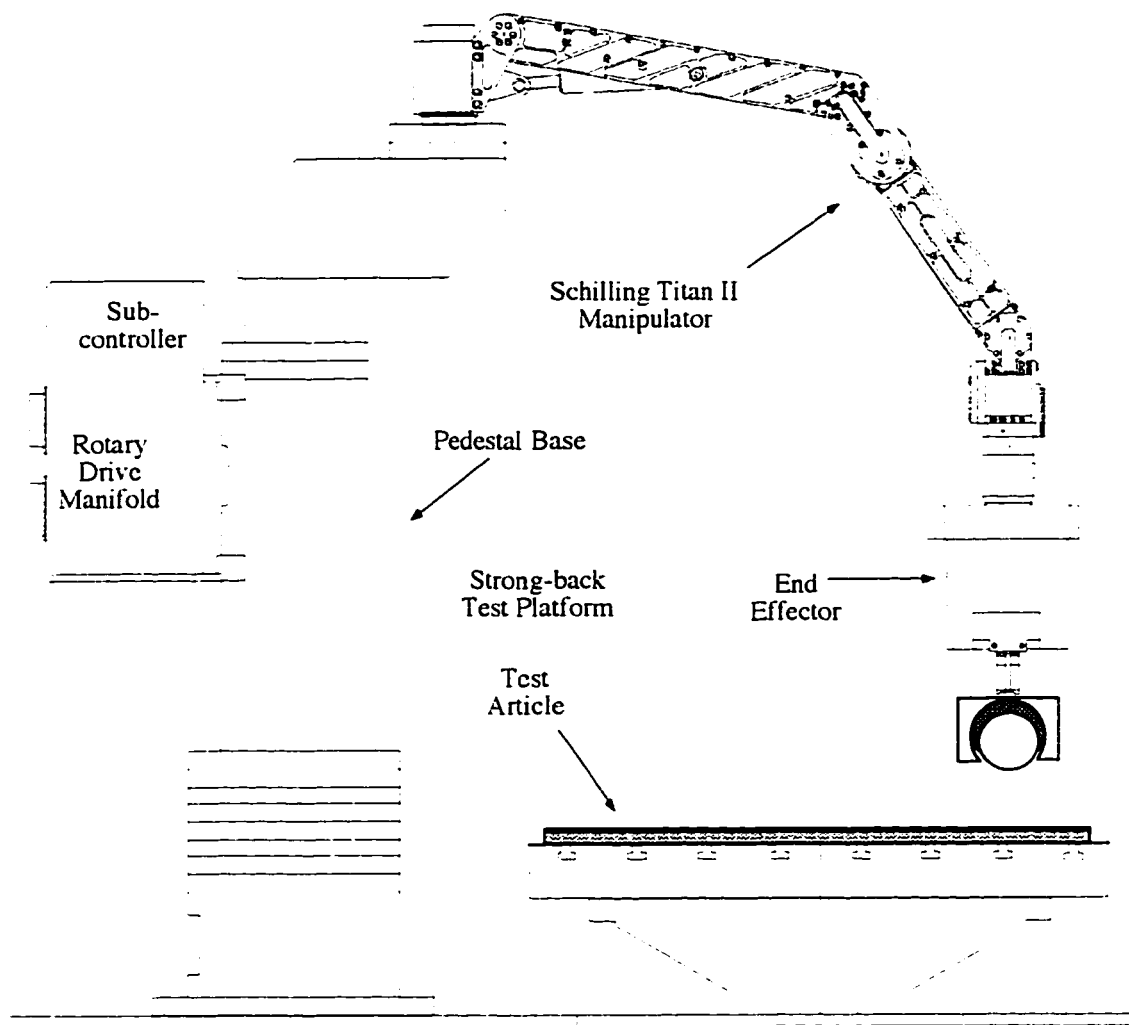


Figure 4-1 Schilling Titan II robot configuration

plate could be raised or lowered to provide contact with the manipulator.

It is assumed that the mass of each link is a point mass located at the mid-point of the links. Throughout the testing experiments, the desired force  $F_d$  is set at 20 lbs, and the position of the environment is known to the robot. During the first 15 seconds of the motion, the arm is moving freely toward the surface (in Z direction). When the end effector reaches



the surface, it undertakes a collision and is forced to move along the surface. The change of velocity resulting from the collision in the Z direction, multiplied by the damping coefficient  $C_m$ , causes a large reaction force between the end effector and surface which is shown in figure 4-5. Then, after about 1.5 seconds the force  $F_e$  begins to follow the desired force  $F_d$  [7,31].

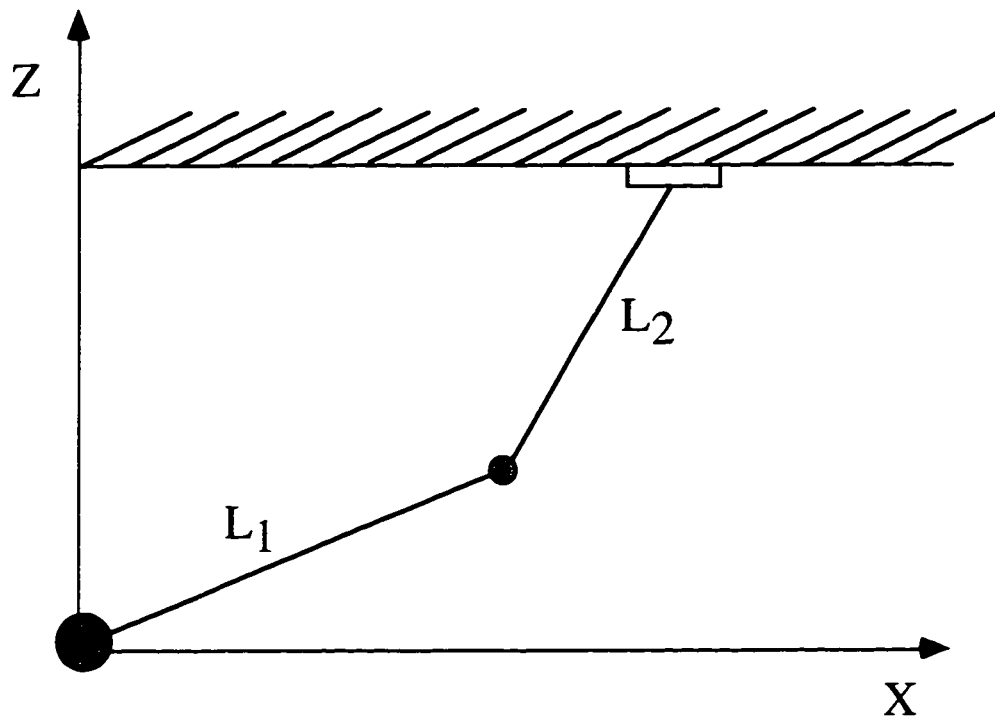


Figure 4-2 Robot-environment force/position coordinate system

The error between  $F_d$  (desired force) and  $F_e$  (actual force) is due to the absence of environment stiffness. Since the ratio  $\alpha=I_r/I_e$  is only 0.02, the error in force is small. The actual force  $F_e$  of robot in experiment is 19.599 lbs-from the sensors read out. Using  $F_e$

and  $F_d$ , we obtain the estimated environment stiffness  $K_e = 1.96 \times 10^4$ . This stiffness is then incorporated in the control input; a more precise force  $F_e = 20.02$  is obtained which is very close to the desired force  $F_d$  [1,7,29,31].

## 4.4.2 Experimental Verification of Target Dynamics

A Schilling Titan II robot made by Schilling Development Inc. was used to perform the experiment, verify the concept, and obtain the results. Schilling is a two-arm serial linkage robot operating in all 6 DOFs. A schematic illustration of the robot is shown in figure 4-1: see appendix A for more details on the Schilling Titan II robot structure and specifications. The manipulator is equipped with a *JR3* force/torque sensor. The force, velocity, and position signals are sampled at 50 Hz and the control signal is recalculated at 50 Hz. The sampling rate is approximately 30 times higher than the bandwidth of the target dynamics. Therefore, we have neglected the effects of time delays. If time delay is an issue, the reader should refer to the work of Lawrence [7,23].

The experiment was performed for two different Force/Moment Accommodation (FMA) threshold settings of 10 and 20 lbs. Translational DOFs (X,Y,Z) are in lbs and rotational DOFs (roll, pitch, yaw) are in in-lbs. The 10 lb setting was done as a system check to verify the control system software and the hardware set up. Although the Schilling is capable of performing in all 6 DOFs, for the purposes of this thesis the experiments were carried out in single DOF at a time. For example, for the first series of tests, the FMA threshold setting was set to 20 lbs in the X direction and 0 lbs and 0 in-lbs in the other 5 DOFs accordingly. For the second series of tests, the FMA was set to 20 lbs in the Y direction and 0 in the other 5 DOFs. The control system is a PID controller with

the control system gains derived and optimized using real time tuning of the system. In deriving the control system gains, it was assumed that there was no cross coupling between different DOFs. However, the experimental results showed that the robot performance was not completely single DOF as it was assumed and there exists a small amount of cross coupling. The results for both cases, 10 lbs and 20 lbs, were compatible and showed the free fall period of the manipulator followed by the interaction (contact) phase between the ball joint roller and the environment.

Figures 4-5 through 4-13 show the system performance. These figures are time vs. force or torque accordingly. The time axes are represented in real time and have the units of seconds. The vertical axes of these figures are force for X, Y, and Z DOFs and torque for roll, pitch, and yaw DOFs in lbs and ft/lbs respectively.

Figure 4-5 shows the overall force profile of the system for the FMA threshold setting of 20 lbs, both free fall and the contact phase. The first segment of figure 4-5 is the free fall phase of the motion for which the manipulator experiences no external forces (force of gravity is compensated for but not measured). The second segment shows the force profile after the collision has been made.

Figure 4-6 shows the force response of the system from time 0 second until the contact is made. During this phase of the experiment, the manipulator is moving freely along the Z-axis with a constant input command of the hand controller. The first segment of this figure, which is the free fall phase of the motion, is very close to a straight line at 0 lbs. As the contact is happening, the sensors on the manipulator start to record the interaction forces; this is shown on the figure.

Figure 4-7 shows the force response of the system after the end effector has made contact with the environment (the table in figure 4-1). Due to the amount of damping available to the system, the transient period is considerably smooth but long. This is because of some operational constraints and time delay between the controller and the robot. The system error is less than 10% of the FMA threshold setting (by looking at this figure). The time axis of figure 4-7 starts from 0 which corresponds to the time that contact takes place. The data for this graph was taken from the sensor cells that are attached to the environment (table), not the end effector; therefore, the sensors do not see any force prior to contact.

Figure 4-8 shows the interaction forces between the end-effector and the environment. This is caused by the end effector going from no contact and no external force free fall to contact motion with the environment. As it can be seen from the figure, the system settles down and damps out very quickly, less than one second. This is because the system has high damping and the arm translational velocity is relatively small, about 0.5 inch per second.

Figures 4-9 through 4-13 show the system performance in Y, Z, roll, pitch, and yaw DOFs, respectively. Theoretically, these graphs should have been straight lines along the time axis at 0 lbs or 0 in-lbs. However, this did not occur due to some disturbances and undesired forces present in the system (more on these anomalies later). The disturbances were expected to be higher during the contact phase of the experiment due to the environment interaction. This is shown on the graphs.

Due to the cross coupling and other anomalies, the forces in the Y, Z, roll, pitch,

and yaw directions were not 0, as they should have been since the motion was one DOF.

Two possible and likely sources of the anomalies are:

- Noise associated with the hardware
- Low accuracy and resolution of the JR3 force/moment sensor

By the above example, it is shown that the interaction forces of an impedance controlled robot can be controlled actually using the methods in section 2.1 and 2.2. Although the robot experiences two different kinds of motion from the free motion to the constraint motion the control input does not change, see Figure 4.3. Also, there is no switching of control modes which is usually needed in most of the present force control schemes.

## 4.5 Conclusion

When an impedance controlled robot manipulator is in contact with the environment, the interaction force is completely determined by its input position, target impedance, and the environment mechanical properties. When the environment is very stiff, force can also be controlled to a desired accuracy range without the environment model. When the stiffness of the environment is not much greater than that of target impedance, it is necessary to estimate the model of the environment to control the interaction force. Considering the robot and the environment as a whole system and using the relationship between the desired force and the interaction force, we obtained the environment model without measuring its deformation. Then the estimated model was used to improve the performance of the force control.

# Input Command to the System

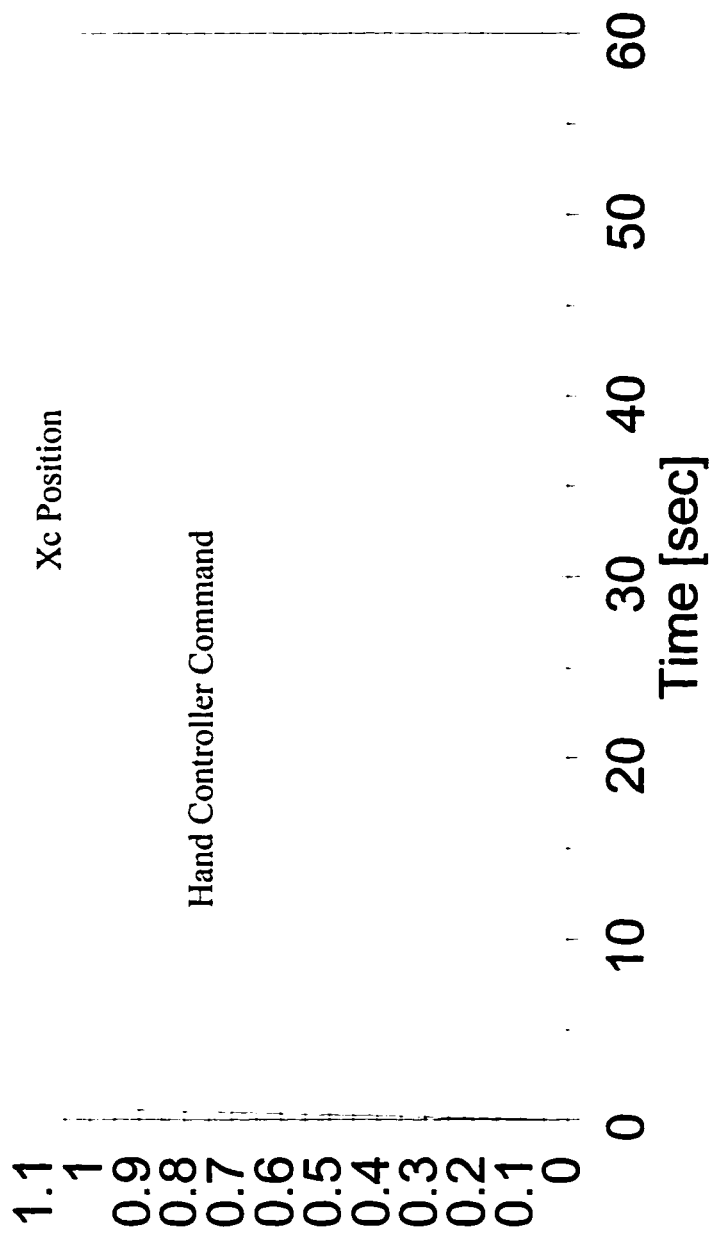


Figure 4-3 Input command to the system

# Input Command to the System

First two seconds

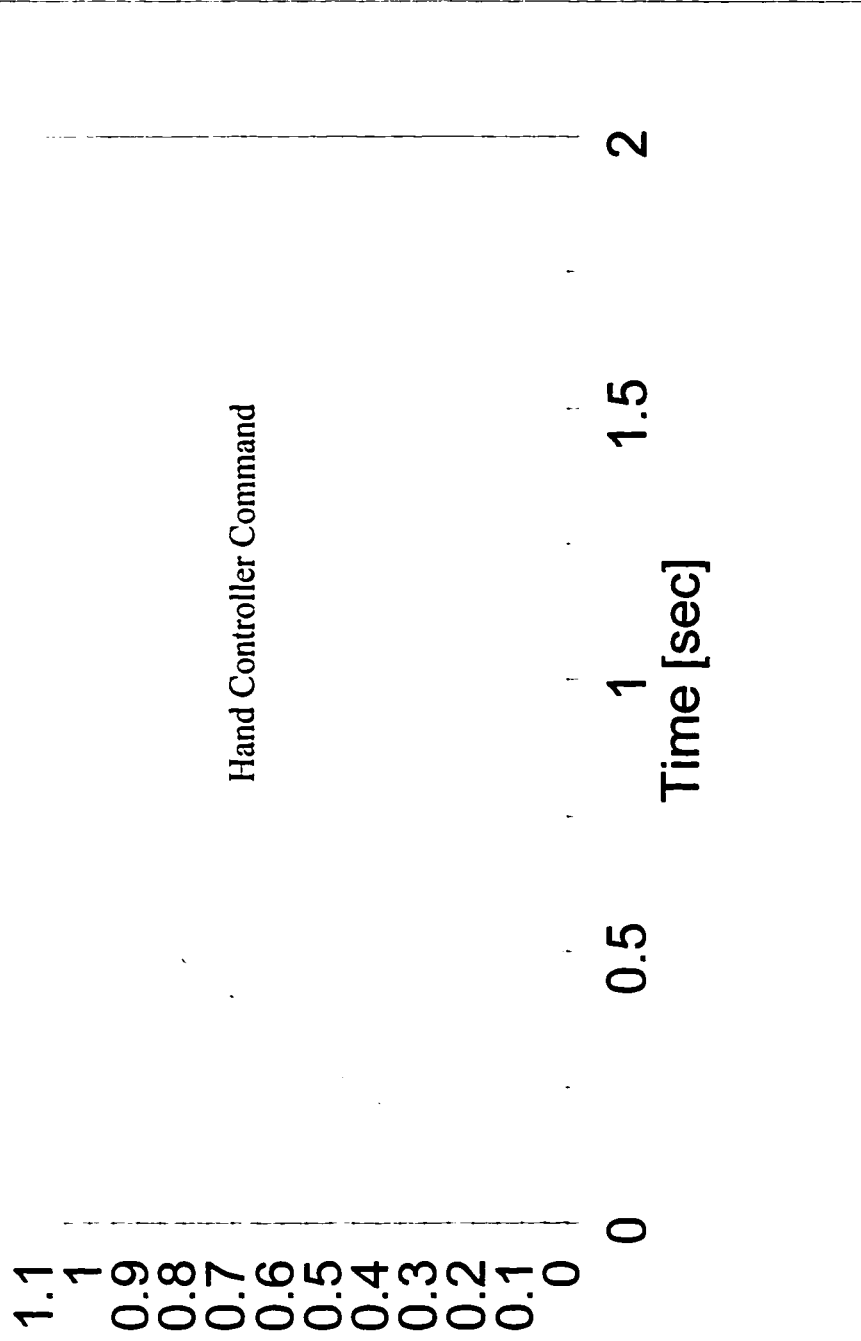


Figure 4-4 Input command to the system-First two seconds

# Overall System Response

FMA = 20.0 lbs

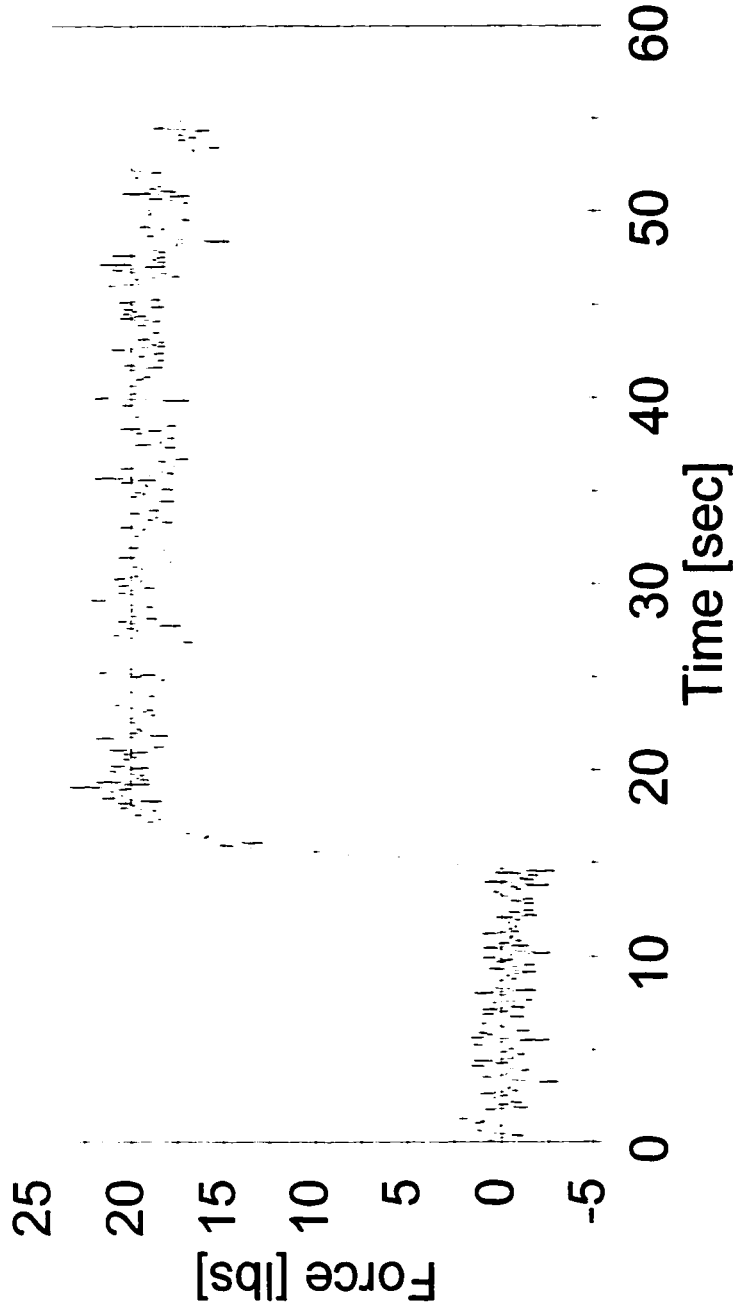


Figure 4-5 Overall system response: both free fall and contact phase



# System Response During Free Fall

Z Forces, FMA = 20 lbs



Figure 4-6 System response free fall in the Z direction

# System Response After Collision

X Forces, FMA = 20 lbs

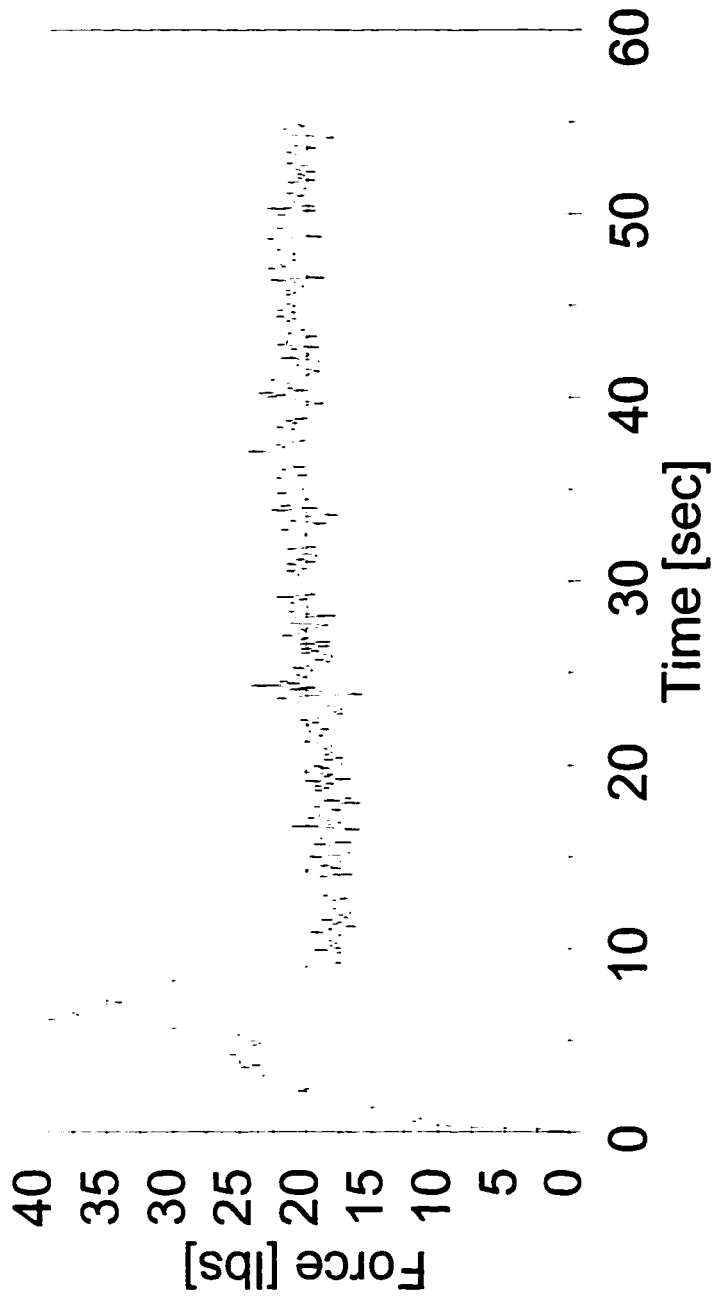


Figure 4-7 System response during the contact phase in the X direction

# Interaction Forces During Collision

FMA Setting = 20 lbs

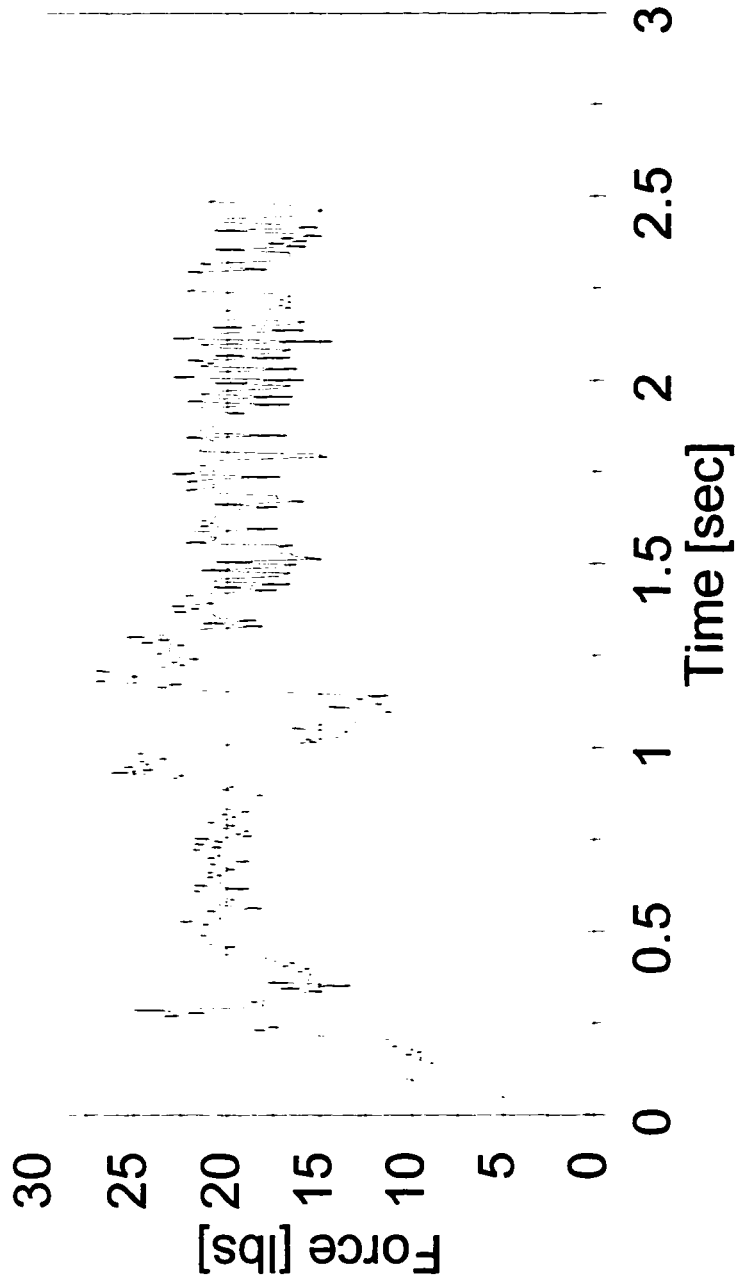


Figure 4-8 Interaction forces during contact

# System Response After Collision

Z Forces, FMA = 0 lbs

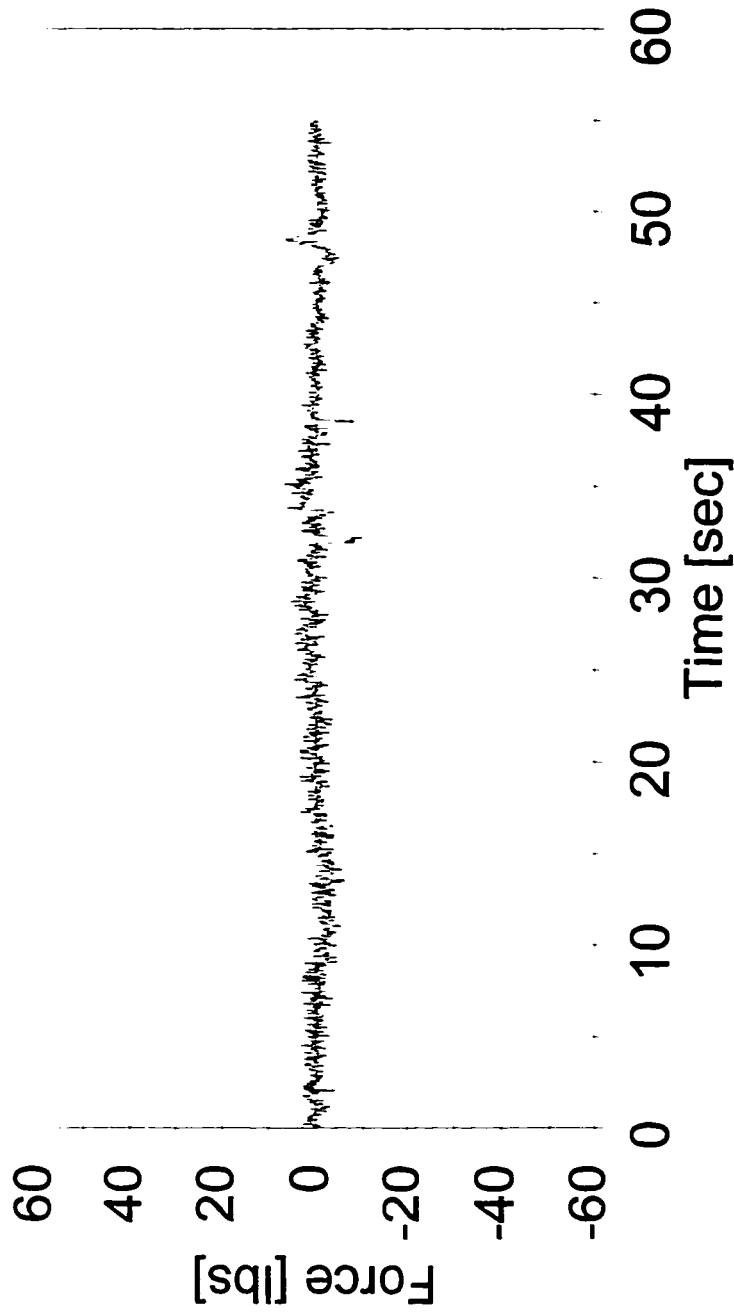


Figure 4-9 Forces in the Z direction after contact

# System Response

Y Forces, FMA = 0 lbs

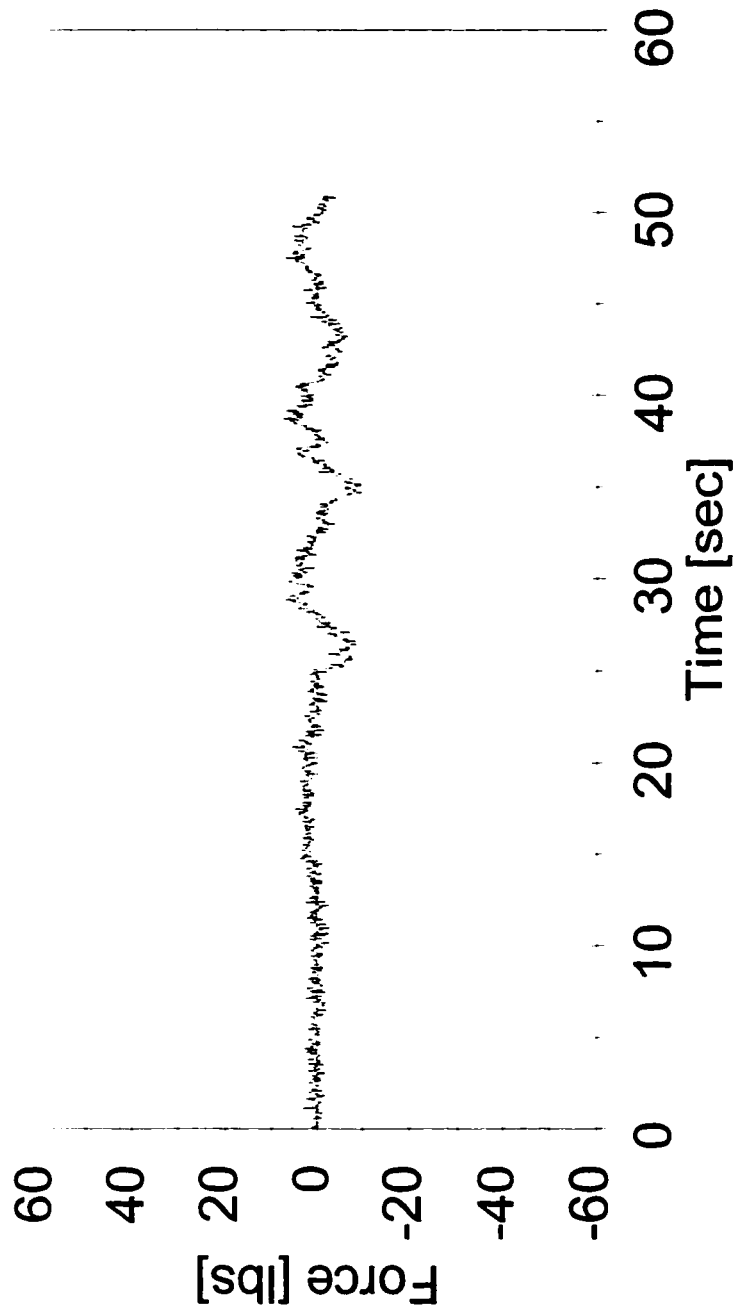


Figure 4-10 Overall forces in the Y direction

# System Response

Pitch, FMA = 0 ft-lbs

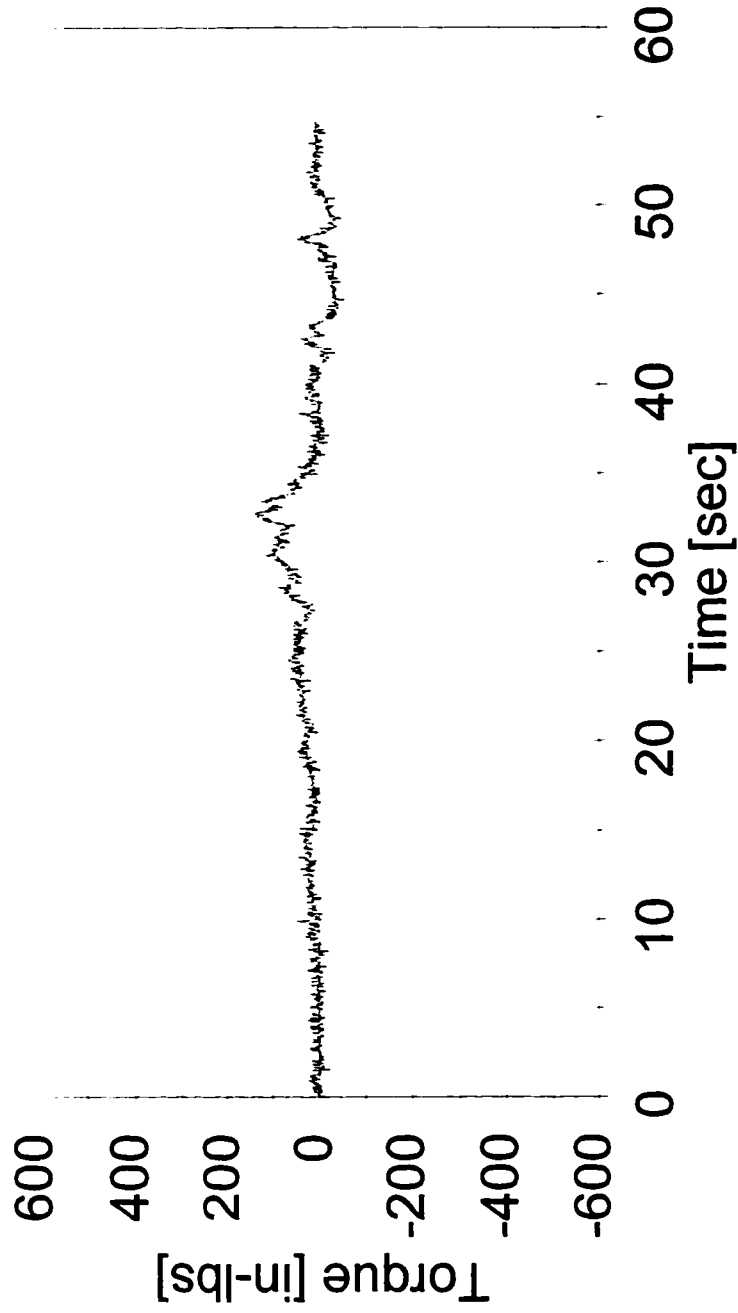


Figure 4-11 Overall torques in the pitch DOF

# System Response

Roll, FMA = 0 ft-lbs

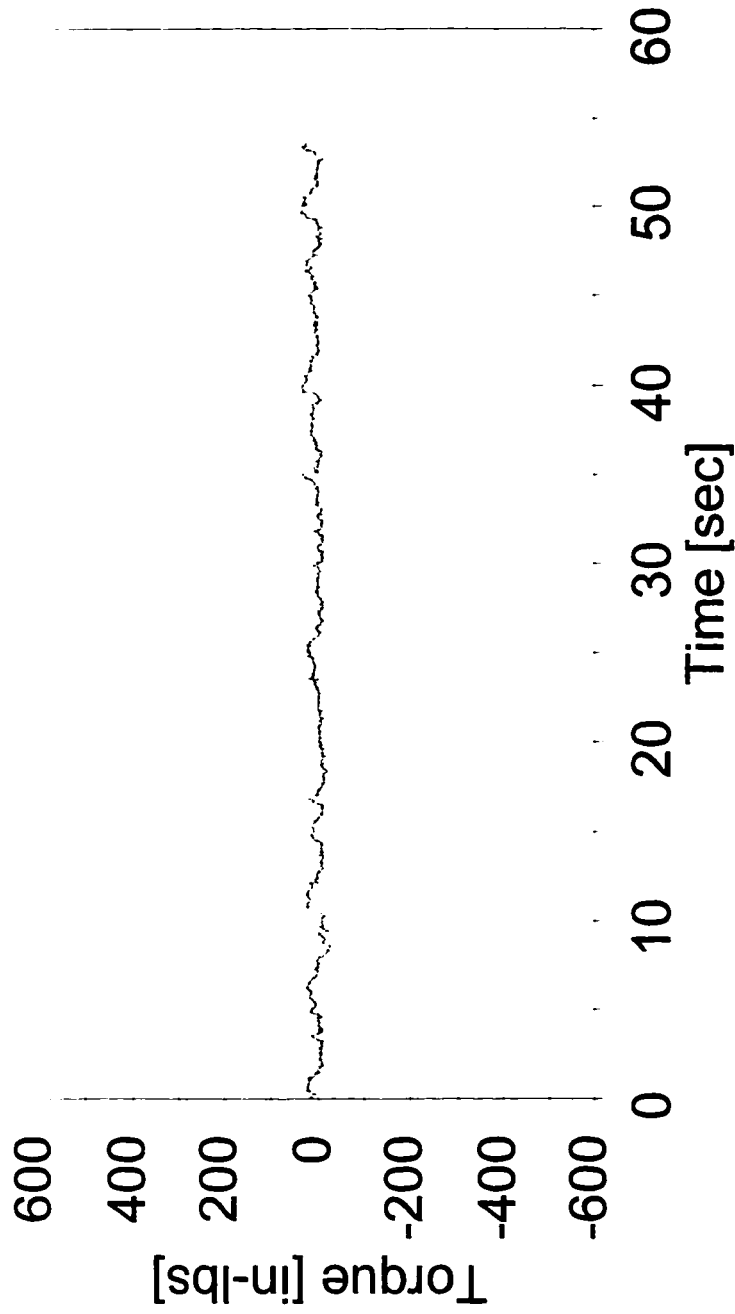


Figure 4-12 Overall torques in the roll DOF

# System Performance

Yaw, FMA = 0 ft-lbs

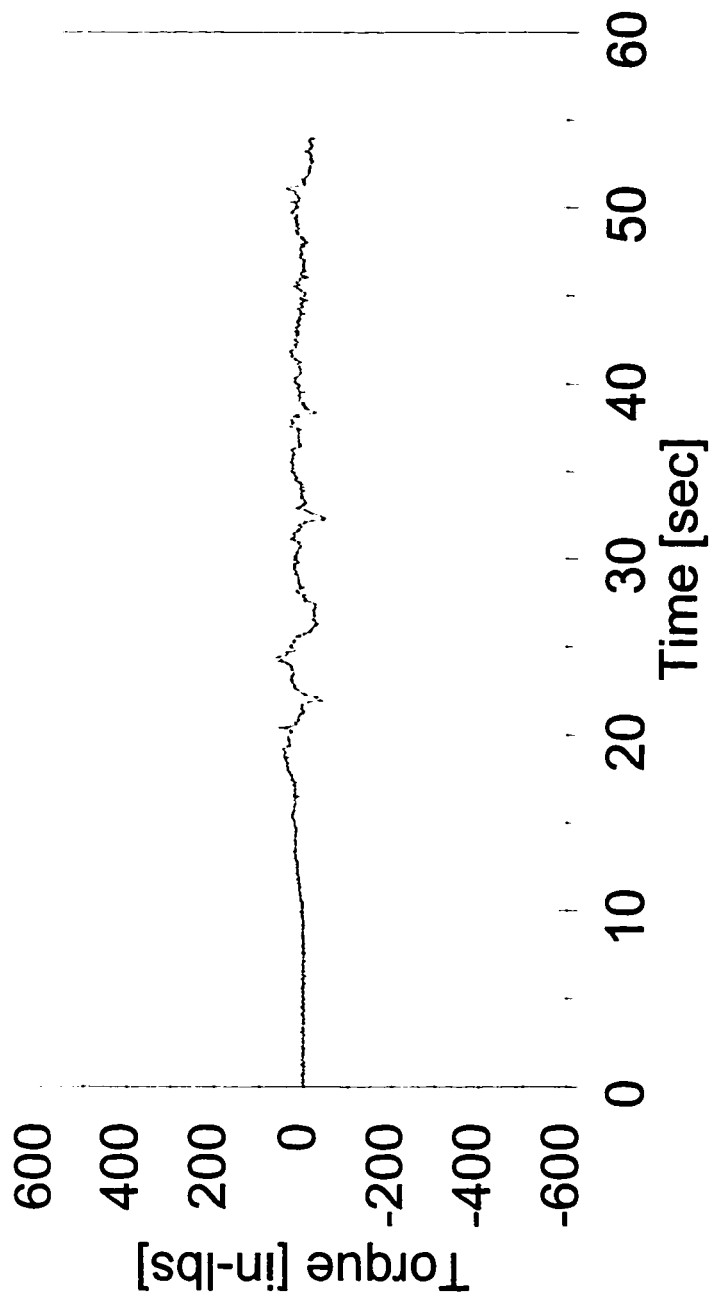


Figure 4-13 Overall torques in the Yaw DOF



# Chapter 5

## Conclusion & Future Work

### 5.1 Conclusion

First, a brief survey of related topics and literature survey has been presented. It clearly shows that the field of robotic dynamics and controls is relatively new. The literature survey also shows that there are many areas that have not been explored yet.

Then, the theory of impedance control is presented in chapter three. This theory considers the effect of manipulator dynamics and the behavior of two primary approaches to impedance control-force based impedance control and position based impedance control. The results are cast in the form of stability boundaries-the relationship between desired impedance parameters and the environment.

Next, the concept of target impedance reference trajectory is introduced which characterizes a desired dynamic relation of end point with the environment. A force based controller is designed to assign a control torque such that the overall system dynamics

coincides with the target impedance. Finally, the system was tested with a Schilling manipulator system. The results showed that the system performance was as expected. The graphs presented in section 4.4.2 clearly represent the trajectory path, applied forces, and the arm behavior of the proposed test plan.

## 5.2 Future Work

The work presented in this thesis can be expanded further more. It will be interesting to simulate the overall system with the aid of some computer software and investigate the compatibility of the simulation results with the experimental results. This work can also be repeated for a position based impedance control and the results can be compared with the force based impedance control presented in this thesis. Another interesting area of expansion is to look into the system from the adaptive point of view. The comparison between the results obtained from above mentioned approaches will reveal the true characteristics and behavior of the system.

# Appendix A

# Schilling manipulator specifications

## A.1 The Test Facility Specification

The robot parameters and specifications discussed in this appendix were obtained from the technical publications furnished by the manufacturer.

The Schilling Titan II is a six DOF hydraulic manipulator that has a 240 lbs payload capacity and a built-in JR3 force/torque sensor. The six functions of the manipulator are: 3 translational (X, Y, Z) and 3 rotational (Pitch, Yaw, Roll)

JR3 Force/torque sensor ratings are as follow:

Rating:

Fx, Fy	1000 lb
Fz	4000 lb
Mx, My, Mz	4000 in-lb

Resolution:

Force	11.8 oz
Moment	1.5 in-lb

The control system hardware currently used for the Schilling Titan II is VMEbus products which include a portable 7 slot VME chassis, two 21-slot VME chassis, four EPC5-486 embedded PCs, three EPC-386 embedded PCs, two dual TMS320C30 Digital Signal Processor modules, two 68010 controlled serial interface cards, five Ethernet interface modules, two PC add-in card adapter modules, four SVGA graphics controller modules, four hard disks, two flash disks, and Dynamic Random Access Memory. They are integrated into workstations and used to operate two Schilling Hydraulic Manipulators. The VME bus based controllers are essentially hierarchical multi processors systems, including C30s as servo processors, 386s as motion processors, 486s as user interface processors, and 486s as teleoperation processors. The current system is setup for the proof-of-concept demonstrations of advanced technology areas.

## A.2 General Description

### Standard Dimensions and Specifications:

Maximum Reach	76.3 in
Lift Capacity (maximum)	1200 lb
Lift Capacity (full extension)	240 lb
Wrist Torque	75 ft-lb(peak)
Jaw Capacity	4.0 in
Weight	175 lb

## A.3 Range of Motion

Waist Yaw	270 <sup>o</sup>
Shoulder Pitch	120 <sup>o</sup>
Elbow Pitch	270 <sup>o</sup>
Wrist Pitch	180 <sup>o</sup>
Wrist Yaw	180 <sup>o</sup>
Wrist Rotate	
Slaved	270 <sup>o</sup>
Continuous	0-55 rpm

## 6.0 References

- [1] W.S. Lu and Q.H. Meng, "Adaptive impedance control of mechanical manipulators", *Robotics and manufacturing recent trends in research, education, and publication*, 1990, pages 329-335.
- [2] H. Kazerooni, "A robust design method for impedance control of constrained dynamics system", *Ph.D. thesis*, Massachusetts Institute of Technology, Department of Mechanical Engineering, 1985.
- [3] W. McCormic and H.M. Schwartz, "An investigation of impedance control for robot manipulators", *The International Journal of Robotic Research*, October 1993, Pages 473-489.
- [4] Neville Hogan, "Impedance control: An approach to manipulation", Parts I, II, and III, *ASME Journal of Dynamic systems, Measurement, and Control*, March 1985, pages 1-24.
- [5] Kennon Guglielmo and Nader Sadegh, "Implementing a hybrid learning force control Scheme", *IEEE Journal of Control Systems*, February 1994, pages 72-79.
- [6] J.J. Craig, *Introduction to robotics: Mechanics and Control*, Reading Mass, Addison-Wesley, 1989.
- [7] Dale A. Lawrence, "Impedance Control Stability Properties in Common", *IEEE International Conference on Robotics and Automation*, January 1985, pages 1185-1190.
- [8] Neville Hogan, "Stable execution of contact tasks using impedance control", *IEEE*

*Conference on Robotics and Automation*, March 1987, pages 1047-1054.

[9] H. Kazerooni and S. Kim, "A new architecture for direct drive robot". *IEEE International Conference on Robotics and Automation*, January 1988, pages 442-445.

[10] N.H. McClamroch and D. Wang, "Feedback stabilization and tracking of constrained robots", *IEEE Transactions on Automatic Control*, vol. 33, no. 5, 1988, pages 419-426.

[11] M.H. Raibert and J.J. Craig, "Hybrid position/force control of manipulators", *ASME Journal of Dynamic Systems, Measurement, and Control*, June 1991, pages 126-133.

[12] Dale.A. Lawrence and R.M. Stoughton, "Position-based impedance control: Achieving stability in practice", *Proceedings of AIAA Conference on Guidance, Navigation, and Control*, August 1987.

[13] T. Yoshikawa, T. Sugie, and M. Tanaka, "Dynamic hybrid position/force control of robot manipulators", *IEEE Transactions on Robotics and Automation*, June 1988, pages 699-705.

[14] C.H. An and J.M. Hollerbach, "Dynamic stability issues in force control of manipulators", *IEEE International Conference on Robotics and Automation*, April 1987, pages 890-896.

[15] S.D. Eppinger and W.P. Seering, "Understanding bandwidth limitations in robot force control", *IEEE International Conference on Robotics and Automation*, April 1987, pages 904-909.

[16] H. Kazerooni, T. Sheridan, and P. Houpt, "Robust compliant motion for manipulators, part I: The fundamental concepts of compliant motion", *IEEE Journal of Robotics and Automation*, 1986, pages 83-91.

[17] E. Colgate and N. Hogan, "Robust control of dynamically interacting systems", *International Journal of Controls*, January 1988, pages 65-88.



- [18] R. Anderson and M. Spong, "Hybrid impedance control of robotic manipulators", *IEEE Journal of Robotics and Automation*, October 1988, pages 549-556.
- [19] L. Mo and M.M. Bayoumi, "Hybrid adaptive impedance control of robot manipulators", *Robotics and manufacturing recent trends in research, education, and publication*, 1990, pages 351-357.
- [20] D.E. Whitney, "Historical perspective and state of the art in robot force control", *IEEE International Conference on Robotics and Automation*, March 1985, pages 262-268.
- [21] O. Khatib, "A unified approach for motion and force control of robot manipulators: the operational space formulation", *IEEE Journal of Robotics and Automation*, February 1987, pages 43-53.
- [22] J.A. Maples and J.J. Becker, "Experiments in force control of robotic manipulators", *IEEE International Conference on Robotics and Automation*, April 1986.
- [23] Dale A. Lawrence and Jim D. Chapel, "Quantative control of manipulator/task interaction", *IEEE Journal of Control Systems*, April 1994, pages 14-25.
- [24] Neville Hogan, "Mechanical impedance control in assistive devices and manipulators", *Proceedings of the Joint Automatic Controls Conference*, Vol. I, San Francisco, August 1980.
- [25] Neville Hogan, "Impedance control of a robotic manipulator", *Winter anual meeting of the American Society of Mechanical Engineers*, Washington, D.C., 1981.
- [26] M. Spong and M. Vidyasagar, *Robot dynamics and control*, John Wiley & sons, New York, 1989.
- [27] John J. Craig, Ping Hsu, and H. Shankar Sastry, "Adaptive control of mechanical manipulators", *International Conference on Robotics and Automation*, February 1986, pages 190-195.
- [28] Neville Hogan, "On the stability of the manipulators performing contact task", *IEEE Journal of Robotics and Automation*, vol RA-4, December 1996, pages 667-686.

- [29] J.Y.S. Luh, M.W. Walker, and R.P. Paul. "Resolved acceleration control of mechanical manipulators", *IEEE Transactions on Automatic Control*, June 1980, pages 468-474.
- [30] J.Y.S. Luh, M.W. Walker, and R.P. Paul, "On-line computational scheme for mechanical manipulators", *ASME Journal of Dynamic systems, Measurement, and Control*, 1980, pages 69-76.
- [31] Zien Lu and A.A. Goldenberg, "Implementation of robust impedance and force control using VSS", *IEEE Journal of Robotics and Automation*, April 1990, pages 279-285.
- [32] Julio J. Gonzalez, Luciano Chirinos, Bruce S. Widman, and Glenn R. Widmann, "A force commanded impedance control scheme for robots with nonlinearities". *Robotics and manufacturing recent trends in research, education, and publication*, 1990, pages 239-244.
- [33] G.J. Liu and A.A. Goldenberg, "Robust Hybrid impedance control of robot manipulators", *IEEE International Conference on Robotics and Automation*, April 1991, pages 274-280.
- [34] Dong Sang Yoo, Han Ho Choi, and Myung Jin Chung, "Adaptive variable structure tracking for robot manipulators," *IEEE Region 10 conference, Tenecon 92*, 11th-13th November, 1992.
- [35] S.P. Chan and Wei-Bing Gao, "Variable structure model-reaching control strategy for robot manipulators", *IEEE International Conference on Robotics and Automation*, August 1989, pages 1504-1508.
- [36] Gang Feng, "An improved adaptive control algorithm for partially known rigid robots", *IEEE Region 10 conference, Tenecon 92*, 11th-13th November, 1992.
- [37] M.R. Cutkosky and I. Kao. "Computing and Controlling Compliance of Robotic Hands" *IEEE Transactions on Robotics and Automation*, 1989.

[38] John Li and I. Kao, "Grasp Stiffness Matrix-Fundamental Properties in Analysis of Grasping and Manipulation", *IROS'95*, 1995